

西藏班公湖—怒江缝合带美日切错组中酸性火山岩锆石 U-Pb 年龄、Sr-Nd-Hf 同位素、岩石成因及其构造意义

韦少港¹⁾, 唐菊兴²⁾, 宋扬²⁾, 刘治博²⁾, 王勤³⁾, 林彬²⁾, 贺文¹⁾, 冯军⁴⁾

1) 中国地质大学(北京)地球科学与资源学院, 北京, 100083; 2) 中国地质科学院矿产资源研究所, 北京, 100037; 3) 成都理工大学, 成都, 610059; 4) 中铝西藏金龙矿业股份有限公司, 拉萨, 850000

内容提要:西藏班公湖—怒江缝合带是我国重要的斑岩铜金矿成矿带, 成矿地质条件极为优越。多龙矿集区是班公湖—怒江缝合带西段典型斑岩—浅成低温热液型铜(金)超大型矿床, 区内广泛分布着美日切错组喷溢相火山岩, 但其岩石成因、源区属性、形成年代及地球化学动力学背景尚不明确。本文对美日切错组安山岩及流纹岩进行锆石 U-Pb 测年, 获得结晶年龄分别为 108.2 ± 2.6 Ma (MSWD=0.39) 和 109.3 ± 2.2 Ma (MSWD=1.70)。矿区安山岩及流纹岩具高硅 ($\text{SiO}_2 = 60.89\% \sim 72.00\%$)、富钾 ($\text{K}_2\text{O} = 3.08\% \sim 5.53\%$)、富碱 ($\text{K}_2\text{O} + \text{Na}_2\text{O} = 6.88\% \sim 8.96\%$)、准铝质—过铝质 ($\text{A/CNK} = 0.92 \sim 1.28$) 特征, 属于高钾钙碱性及钾玄岩系列岩石。其明显均富集轻稀土(LREE)及大离子亲石元素(LILE: Th、U、K、Pb 及 Rb), 亏损重稀土(HREE)及高场强元素(HFSE: Ta、Nb、Ti 及 Zr), 稀土总量 (ΣREE) 为 $141.52 \times 10^{-6} \sim 236.05 \times 10^{-6}$ 之间, $\text{La}_{\text{N}}/\text{Yb}_{\text{N}}$ 为 $10.42 \sim 11.05$, δEu 为 $0.65 \sim 0.80$, 具有中等负铕异常, 显示出典型岛弧岩浆岩的特征。 $(^{87}\text{Sr}/^{86}\text{Sr})_{\text{i}}$ 值为 $0.7050 \sim 0.7053$, $(^{143}\text{Nd}/^{144}\text{Nd})_{\text{i}}$ 为 $0.5124 \sim 0.5126$, $\epsilon_{\text{Nd}}(t)$ 值为 $-1.51 \sim 1.29$, 具有高 Sr 低 Nd 的特征。锆石 Hf 同位素分析结果表明, 流纹岩 $\epsilon_{\text{Hf}}(t)$ 为 $+11.6 \sim +15.5$, 平均值为 $+13.8$, 两阶段模式年龄平均值为 288.0 Ma; 安山岩 $\epsilon_{\text{Hf}}(t)$ 为 $+3.4 \sim +8.0$, 平均值为 $+4.8$, 两阶段模式年龄平均值为 813.1 Ma; 表现出明显的幔源特征。综合研究表明, 美日切错组火山岩为班公湖—怒江新特斯洋洋壳向北的俯冲背景下, 由俯冲板片脱水产生流体交代地幔楔发生部分熔融形成原始玄武质岩浆, 并在上升后, 滞留在壳幔边界形成新生下地壳, 新生下地壳与持续底侵慢源玄武质岩浆混合而部分熔融形成。其形成于典型岛弧的构造背景下, 暗示班公湖—怒江洋在早白垩世晚期 (108~109 Ma) 仍正在向北俯冲于羌塘地块之下, 可能尚未关闭。

关键词:闭合时限; 岛弧火山岩; 美日切错组; 班公湖—怒江成矿带西段; 西藏

班公湖—怒江成矿带地跨青藏高原中部班公湖—怒江缝合带(下简称“班怒带”)两侧, 是青藏地区继玉龙成矿带和冈底斯成矿带之后发现的第三条斑岩铜金成矿带(Tang Juxing et al., 2014; Cui Ning et al., 2016; Sun Zhenming et al., 2015)。班怒带西起(印控)克什米尔, 经日土—改则—班戈—东巧—丁青呈近东西向展布, 在嘉玉桥处折向东南, 沿怒江一路延伸至滇西, 总长约 2400 km, 总面积约 12.34×10^4 km 2 , 呈“S”型带状横亘于青藏高原中部。中生代班公湖—怒江洋发生俯冲—碰撞造山作

用, 诱发了燕山期大规模岩浆活动, 伴有大规模的岩浆岩侵入作用及火山喷发作用; 缝合带沿线可见许多蛇绿混杂体, 发现有金、铜、铬等金属矿(床)点成带状展布(Qu Xiaoming et al., 2006)。该成矿带的西段构造—岩浆带成矿地质条件极为优越, 发育了包括尕尔穷—嘎拉勒斑岩—矽卡岩型铜金矿、弗野—材玛矽卡岩型磁铁矿及多不杂—铁格隆南(以下简称“多龙矿集区”)斑岩—浅成低温热液型铜(金)矿床等多个超大型或大型矿床(图 1a)。多龙矿集区地处班公湖—怒江缝合带西段北侧的南羌塘南

注: 本文受国土资源部公益性行业专项“斑岩—浅成低温热液成矿系统研究及勘查评价示范—以西藏多龙整装勘查区为例”(编号: 201511017)、国家自然科学青年基金“西藏羌塘地体南缘铁格隆南超大型浅成低温热液型铜(金)矿床保存条件研究”(编号: 41402178) 及科技基础性工作专项(项目编号: 2014FY121000)共同资助。

收稿日期: 2015-11-17; 改回日期: 2016-05-24; 责任编辑: 黄敏。

作者简介: 韦少港, 男, 壮族, 1989 年生, 博士, 矿产普查与勘探专业, Email: 634719227@qq.com。

通讯作者: 唐菊兴, 男, 1964 年生, 博士, 研究员, 从事矿床学和固体矿产勘查与评价研究工作, Email: tangjuxing@126.com。

缘,发育西藏首例典型斑岩—浅成低温热液型铜(金)矿床超大型矿床,引起了众多学者的广泛关注(Chen Huaan et al., 2013; Fang Xiang et al., 2015; Li Guangming et al., 2007; Li Jinxiang et al., 2008; Li et al., 2011a, 2011b, 2012, 2013 and 2014a; Qu Xiaoming et al., 2006; She Hongquan et al., 2009; Tang Juxing et al., 2014; Xin Hongbo et al., 2009; Yang Chao et al., 2015; Zhu Xiangping et al., 2015; Zhu et al. 2015)。但是对于大面积出露的美日切错组火山岩(图 1b),目前只有针对高 Nb 玄武岩及玄武安山岩等(偏)基性火山岩的有限报道(Li Jinxiang et al., 2008; Wang Qin et al., 2015),对于安山岩、流纹岩等中酸性火山岩还缺乏地球化学数据及高质量地质年代学报道。从而导致对美日切错组火山岩的岩石成因、形成环境及地球动力学背景一直未能理清,对班公湖—怒江洋盆碰撞闭合的时限存在着从早侏罗世(J_1)到早白垩世(K_1)的争议(Duan Zhiming et al., 2013; Kapp et al., 2003; Zhu Dicheng et al., 2006a, 2006b)。

因此,本文主要目的是,首先分析笔者获得的美日切错组中酸性火山岩样品的性质、岩石地球化学、地质年代学及其同位素地球化学特征,结合前人中已取得的地球化学数据,初步讨论班公湖—怒江新特提斯洋演化可能涉及的地球动力学过程。

1 区域地质背景及样品采集

研究区位于西藏改则县北西约 120km 处,大地构造位置处于羌塘—三江复合板片南缘,班公湖—怒江缝合带西段北侧。以班公湖—怒江缝合带为界,北部属于羌塘—三江复合板片,南部属于冈底斯—念青唐古拉板片。班公湖—怒江缝合带以零散分布的蛇绿岩残片为标志(Shi R D, 2007),是青藏高原的地质构造和深部地球物理反映的岩石圈结构和组成的非常重要的分界线,是拉萨地块和羌塘地块的分界(Yin and Harrison, 2000),也可能是冈瓦纳板块的北界(Pan Guitang et al., 2004)。区内出露地层为上三叠统日干配错组(T_3r)、下侏罗统曲色组(J_1q)、中下侏罗统色哇组($J_{1-2}s$)、下白垩统美日

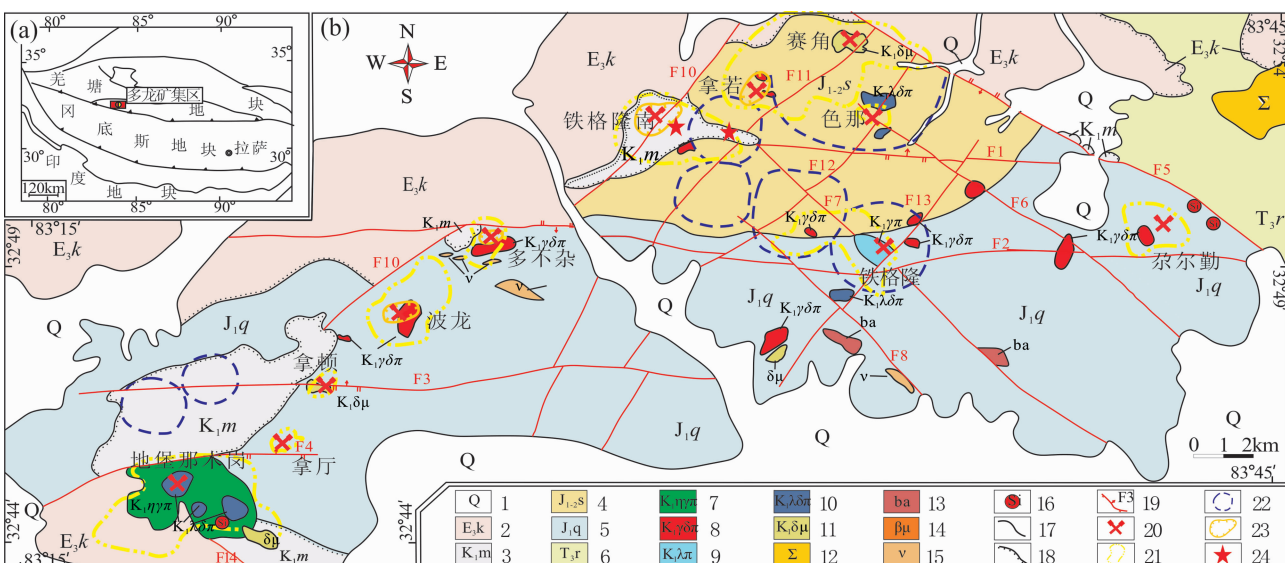


图 1 西藏多龙矿集区区域地质图(据 Yang Chao et al., 2015 修改)

Fig. 1 Regional map of the Duolong deposit, Tibet(After Yang Chao et al. , 2015)

1—第四系;2—上渐新统康托组;3—下白垩统美日切错组;4—中下侏罗统色哇组;5—下侏罗统曲色组;6—上三叠统日干配错组;7—早白垩世二长花岗斑岩;8—早白垩世花岗闪长斑岩;9—早白垩世石英斑岩;10—早白垩世石英闪长斑岩;11—早白垩世闪长斑岩;12—蛇纹石化橄榄岩;13—枕状玄武岩;14—辉绿岩;15—辉长岩;16—硅帽;17—整合接触界线;18—不整合接触界线;19—断层及编号;20—矿床位置;21—地表冲积带范围;22—遥感影像提取的环形构造;23—工程控制矿体范围;24—取样位置

1—Quaternary; 2—Upper Oligocene Kangtuo Formation; 3—Lower Cretaceous Meiritiecuo Formation; 4—Lower-Middle Jurassic Sewa Formation; 5—Lower Jurassic Quse Formation; 6—Upper Triassic Riganpeicuo Formation; 7—Early Cretaceous monzonitic granite porphyry; 8—Early Cretaceous granodiorite porphyry; 9—Early Cretaceous quartz porphyry; 10—Early Cretaceous quartz diorite porphyrite; 11—Early Cretaceous dioritic porphyrite; 12—serpentinized olivinite; 13—pillow basalt; 14—diabase; 15—gabbro; 16—silicification cap; 17—conformity boundary; 18—unconformity boundary; 19—fault and number; 20—positon of mines; 21—alteration scope at surface; 22—the ring structure of remote sensing image; 23—controlled ore body scope; 24—positon of samples

切错组(K_1m)、上渐新统康托组(E_3k)和第四系(图1)。上三叠统日干配错组为灰岩。下侏罗统曲色组为次深海陆棚—盆地斜坡复陆碎屑岩—类复理石建造,主要岩性为长石石英砂岩、粉砂岩夹硅质岩、夹有灰绿色玄武岩、英安岩等;中下侏罗统色哇组为深灰、灰色薄层状粉砂岩、中层长石石英砂岩、石英砂岩与灰白色薄层状泥质板岩互层。下白垩统美日切错组主要为安山岩、安山质玄武岩。上渐新统康托组为砂砾石层、砾岩含砾砂岩(Fang Xiang et al., 2015)。研究区南部的班公湖—康托—兹格当错为超壳断裂,是羌塘地块和冈底斯—念青唐古拉板片的分界,也是班公湖—怒江缝合带的北界,早期具北向俯冲推覆性质,晚期则具南向逆冲推覆性质。受该断裂的影响,区内断裂构造显著,主要发育有三组,早期近EW向断裂构造F1、F2、F3;后期NE向断裂F8、F10、F11、F12、F13;晚期NW向断裂F4、F5、F6、F7。几组构造呈似菱形格架(图1b),其中NE向断裂为主要的控岩构造,多数含矿斑岩体沿该断裂呈串珠状产出。区内已发现的矿床均沿该方向断裂呈NE向分布。区内断裂构造非常发育,为岩浆的上侵提供良好条件。区内岩浆活动十分频繁、强烈,总体上以喷发、喷溢及超浅成侵入为主,基

性、中酸性、酸性岩体均有出露,规模一般较小,往往是成带状、串珠状展布,成群出现,受断裂构造的控制明显,具多期活动特征(Yang Chao et al., 2015)。

本文安山岩及流纹岩样品均采自美日切错组(K_1m)地层(图1b)。美日切错组火山岩主要沿地堡那木岗—拿厅—拿顿一波龙—多不杂—铁格陇南—拿若—色那一赛角—尕尔勤一线,分别呈北东向和北西向展布,常呈不规则状、岩瘤状或串珠状分布。岩石类型以玄武安山岩—安山岩为主,发育玄武岩—玄武安山岩—安山岩—流纹岩等陆相喷发—溢流相岩石组合。喷发类型为裂隙式喷发(以拿若北西山麓为代表)和中心式喷发(以铁格隆南矿区为代表)。该套火山岩与下伏中侏罗统色洼组(J_2s)地层呈角度不整合接触,并角度不整合位于上渐新统康托组(E_3k)地层之下。流纹岩呈灰色,具流纹构造,斑晶约占20%,以长石、石英为主,长石蚀变强烈,延流纹呈定向排列。安山岩呈暗红色—紫红色,块状构造,镜下见斑状结构;斑晶(15%~25%)主要为斜长石、辉石及少量石英,斜长石斑晶呈长板状或柱状,颗粒大小不一,镜下长度从0.5~1.0 mm不等,可见聚片双晶及卡斯巴双晶,部分绢云母

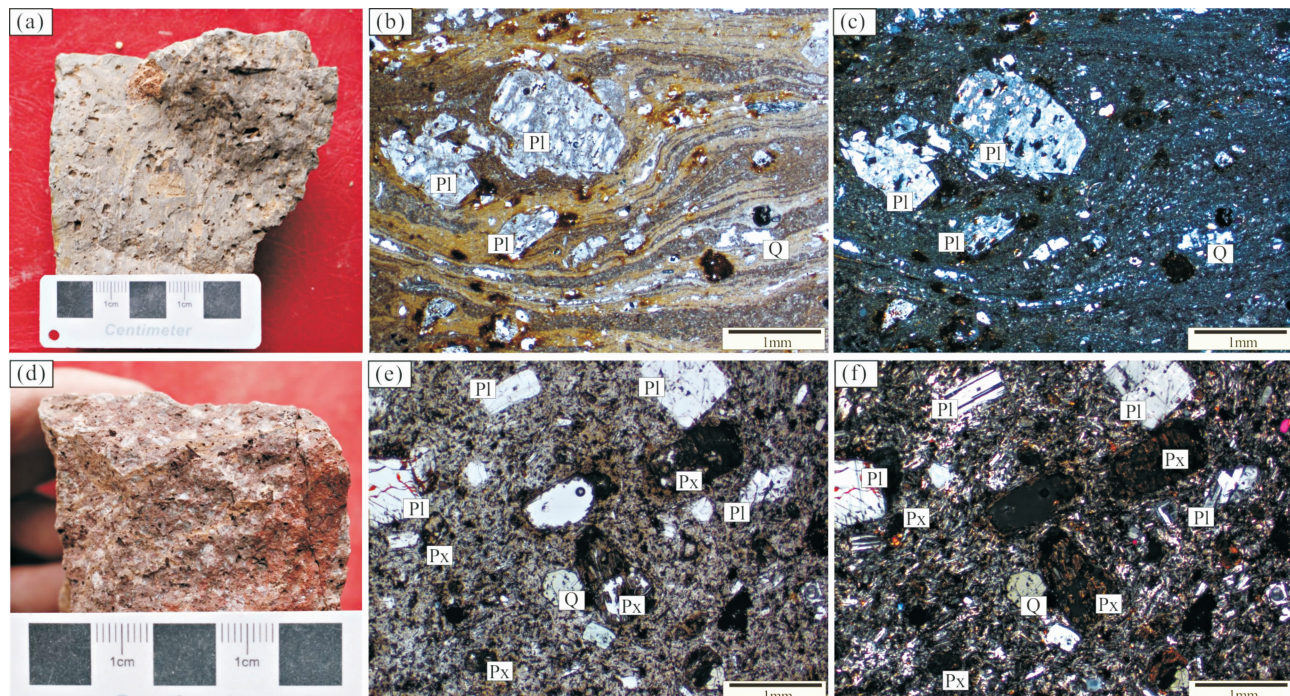


图2 西藏班怒带美日切错组火山岩手标本及显微照片

Fig. 2 Photos of the volcanic rocks from the Meiriqiecuo Fomation in the Bangonghu-Nujiang suture zone, Tibet

(a), (b) and (c)—流纹岩, (d), (e) and (f)—安山岩; Q—石英; Pl—斜长石; Px—辉石

(a), (b) and (c)—Rhyolite, (d), (e) and (f)—Andesite; Q—Quartz; Pl—Plagioclase; Px—Pyroxene

化;石英斑晶发育熔蚀环边,且部分斑晶边缘熔蚀呈港湾状;辉石斑晶多呈粒状或短柱状,粒径从 2.0~1.0 mm 不等,蚀变强烈;基质(75%~85%)见霏细结构或霏细—交织结构,成分为微晶斜长石及少量钛铁矿、磁铁矿等副矿物(图 2)。

2 测试方法

2.1 LA-MC-ICP-MS 锆石 U-Pb 定年

锆石由河北廊坊市宇能岩石矿物分选技术服务有限公司按照标准流程挑选,将选好的待测锆石颗粒置于环氧树脂制靶并刨光,通过锆石透射光、CL 照相分析后选择无包裹体及裂隙部位进行选点,待测。LA-MC-ICP-MS 锆石 U-Pb 定年在中国地质科学院矿产资源研究所 MC-ICP-MS 实验室完成。其中锆石定年分析所采用的仪器为 Finigan Neptune 型 MC-ICP-MS 及与之配套的 Newwave UP 213 激光剥蚀系统。激光剥蚀所用的斑束直径为 25 μm,频率为 10 Hz,能量密度约为 2.5 J/cm²,以 He 为载气。锆石 U-Pb 定年以锆石 GJ-1 为外标,U、Th 含量以锆石 M127(U:923×10⁻⁶; Th:439×10⁻⁶; Th/U:0.475)为外标(Nasdala et al., 2008)进行校正。数据处理和谐和图绘制采用 ICPMSDataCal 和 Isoplot 3.0 程序(Liu et al., 2010)获得。详细实验测试过程可参见 Hou Kejun et al. (2009)。

2.2 全岩地球化学测试

本文地球化学样品的主量元素、微量元素和稀土元素的分析的测试分析在北京核工业地质分析研究中心完成。常量元素用 PHILLIPS PW-2404 型 X-荧光光谱仪分析完成,精度好于 1%;微量元素和稀土元素用 ICP-MS 法测定,仪器型号为 ELEMENT-2 质谱仪,分析精度好于 2%,分析流程见 Qu et al. (2004)的文献。

2.3 Sr-Nd 稳定同位素

全岩 Sr-Nd 同位素分离提取和测量在中国地质大学地质过程与矿产资源国家重点实验室完成,首先准确称量实验要求的全岩粉末(<200 目)50~100 mg,使用纯化 HF-HNO₃-HCl 溶样,之后加入纯化 HCl 使用 Rb-Sr(AG50W-X12, 200~400 目)、Sm-Nd(LN 树脂)交换柱进行分离提纯和元素提取。样品测试仪器型号为热电离质谱仪 TIMS,数据以⁸⁶Sr/⁸⁸Sr=0.1194 和¹⁴⁶Nd/¹⁴⁴Nd=0.7219 校正作为分馏修正。在样品测试的整个过程中,所测定的 Alfa Nd 标样和 NBS-987 Sr 样品的 Nd-Sr

同位素比值,分别为¹⁴³Nd/¹⁴⁴Nd=0.512433±0.000008(±2σ) 和⁸⁷Sr/⁸⁶Sr=0.710252±0.000015(±2σ)。

2.4 锆石 Lu-Hf 同位素

锆石原位 Lu-Hf 同位素分析在西北大学大陆动力学国家重点实验室完成。仪器为 193 nm ArF 准分子激光器的 Nu Plasma 型 MC-ICP-MS。分析采用的激光束直径为 44 μm,剥蚀频率为 8 Hz。具体分析方法及仪器参数见参考文献 Yuan et al. (2008)。

3 分析结果

3.1 形成年代

本文对 1 个流纹岩和 1 个安山岩样品进行锆石 U-Pb 定年。根据锆石 CL 形态特征,美日切错组中酸性火山岩锆石均无色透明,自形程度较好。锆石主要为无色长柱状晶体,少量呈短柱状,其长轴长度为 50~280 μm,长短轴之比多为 2:1~3:1,具有明显的震荡环带(图 3)。仅少数样品含有继承锆石(Hanchar et al., 1993)。

流纹岩样品(DL2014-73)共完成 21 点分析,除 1 号点和 16 号点偏离谐和线较远,予以剔除外,其余 19 个测点数据代表本次岩浆事件。这 19 个分析点的 Th 含量变化在 79.9×10⁻⁶~756.0×10⁻⁶ 之间,U 含量介于 132.7×10⁻⁶~650.4×10⁻⁶ 之间;且 Th 和 U 之间具有明显的正相关性(图略),Th/U 为 0.60~1.16,平均值为 0.75,远大于 0.1(表 1),显示了典型岩浆锆石特征。样品(DL2014-73)的 19 个测点获得的²⁰⁶Pb/²³⁸U 年龄加权平均结果为 109.3±2.2 Ma, MSWD 为 1.70,代表了美日切错组流纹岩的结晶年龄。安山岩样品(DL2014-85)共完成 21 点分析,将偏离谐和线较远的测点予以剔除,其余 14 个测点数据代表本次岩浆事件。这 14 个分析点的 Th 含量变化在 114.4×10⁻⁶~398.1×10⁻⁶ 之间,U 含量介于 160.2×10⁻⁶~354.5×10⁻⁶ 之间;且 Th 和 U 之间具有明显的正相关性(图略),Th/U 为 0.80~1.12,平均值为 0.83,远大于 0.1(表 1),显示了典型岩浆锆石特征。样品(DL2014-85)的 14 个测点²⁰⁶Pb/²³⁸U 获得的加权平均年龄值为 108.2±2.6 Ma, MSWD 为 0.39,代表了美日切错组安山岩的结晶年龄。

3.2 主、微量元素

美日切错组火山岩的主量、微量元素分析结果列于表 2。由表 2 可以看出,火山岩的 SiO₂ 含

表 1 西藏班怒带美日切错组火山岩锆石 U-Pb 年龄数据

Table 1 Zircon U-Pb isotope data of the volcanic rocks from the Meiriqiecu Fomation in the Bangonghu-Nujiang suture zone, Tibet

测点号	含量($\times 10^{-6}$)		Th/U	$^{207}\text{Pb}/^{206}\text{Pb}$		$^{207}\text{Pb}/^{235}\text{U}$		$^{206}\text{Pb}/^{238}\text{U}$		$^{207}\text{Pb}/^{206}\text{Pb}$		$^{207}\text{Pb}/^{235}\text{U}$		$^{206}\text{Pb}/^{238}\text{U}$	
	Th	U		比值	1σ	比值	1σ	比值	1σ	年龄(Ma)	1σ	年龄(Ma)	1σ	年龄(Ma)	1σ
DL2014-73-2	79.9	132.7	0.60	0.0600	0.0176	0.1185	0.0233	0.0168	0.0014	605.6	533.3	113.7	21.1	107.7	9.0
DL2014-73-3	162.7	222.0	0.73	0.0527	0.0055	0.1213	0.0117	0.0172	0.0005	316.7	240.7	116.2	10.6	110.1	3.0
DL2014-73-4	756.0	650.4	1.16	0.0503	0.0050	0.1219	0.0121	0.0177	0.0005	209.3	211.1	116.8	10.9	112.8	3.0
DL2014-73-5	213.8	259.6	0.82	0.0496	0.0152	0.1188	0.0400	0.0172	0.0009	176.0	592.5	114.0	36.4	110.1	6.0
DL2014-73-6	120.9	178.5	0.68	0.0545	0.0060	0.1189	0.0195	0.0164	0.0012	390.8	248.1	114.1	17.7	105.2	7.5
DL2014-73-7	195.4	253.1	0.77	0.0527	0.0050	0.1216	0.0119	0.0169	0.0005	316.7	218.5	116.5	10.7	108.0	3.0
DL2014-73-8	125.3	186.9	0.67	0.0517	0.0080	0.1121	0.0178	0.0157	0.0007	276.0	318.5	107.9	16.2	100.6	4.7
DL2014-73-9	96.1	141.0	0.68	0.0511	0.0106	0.1249	0.0346	0.0180	0.0012	242.7	420.0	119.5	31.2	114.9	7.9
DL2014-73-10	143.6	192.7	0.75	0.0501	0.0067	0.1045	0.0143	0.0153	0.0005	211.2	272.2	100.9	13.1	98.2	3.2
DL2014-73-11	103.9	152.1	0.68	0.0518	0.0091	0.1215	0.0203	0.0174	0.0006	279.7	359.2	116.4	18.4	111.2	3.6
DL2014-73-12	164.9	193.1	0.85	0.0498	0.0056	0.1185	0.0141	0.0169	0.0006	183.4	244.4	113.7	12.8	108.3	3.5
DL2014-73-13	175.7	240.9	0.73	0.0505	0.0081	0.1299	0.0200	0.0188	0.0007	220.4	333.3	124.0	17.9	119.8	4.4
DL2014-73-14	196.4	288.8	0.68	0.0512	0.0035	0.1191	0.0080	0.0169	0.0003	250.1	189.8	114.3	7.2	108.3	1.8
DL2014-73-15	128.5	182.9	0.70	0.0544	0.0055	0.1229	0.0111	0.0171	0.0004	387.1	229.6	117.7	10.1	109.2	2.3
DL2014-73-17	142.0	187.8	0.76	0.0499	0.0085	0.1254	0.0205	0.0181	0.0006	190.8	355.5	119.9	18.5	115.9	3.7
DL2014-73-18	113.1	161.4	0.70	0.0524	0.0084	0.1178	0.0187	0.0167	0.0007	301.9	333.3	113.0	17.0	106.8	4.7
DL2014-73-19	97.6	139.7	0.70	0.0510	0.0097	0.1223	0.0287	0.0174	0.0010	239.0	388.8	117.2	26.0	111.3	6.3
DL2014-73-20	162.1	218.0	0.74	0.0516	0.0078	0.1237	0.0172	0.0179	0.0008	333.4	250.0	118.5	15.6	114.2	4.8
DL2014-73-21	161.2	187.7	0.86	0.0480	0.0073	0.1171	0.0189	0.0176	0.0005	98.2	335.1	112.4	17.2	112.3	3.3
DL2014-85-1	114.4	185.8	0.62	0.0527	0.0083	0.1170	0.0142	0.0170	0.0011	322.3	316.6	112.4	12.9	109.0	7.1
DL2014-85-2	116.6	211.0	0.55	0.0500	0.0060	0.1120	0.0123	0.0165	0.0006	194.5	259.2	107.8	11.2	105.6	4.0
DL2014-85-4	177.3	209.8	0.85	0.0460	0.0062	0.1153	0.0225	0.0167	0.0015	88.6	233.2	110.8	20.5	106.6	9.2
DL2014-85-5	120.9	180.5	0.67	0.0434	0.0120	0.1163	0.0365	0.0159	0.0016	292.3	355.5	111.7	33.3	101.8	9.9
DL2014-85-7	156.0	188.5	0.83	0.0472	0.0062	0.1153	0.0124	0.0173	0.0012	57.5	285.2	110.8	11.3	110.6	7.8
DL2014-85-10	128.0	160.2	0.80	0.0548	0.0088	0.1143	0.0132	0.0165	0.0007	405.6	322.2	109.8	12.0	105.2	4.2
DL2014-85-11	153.6	177.1	0.87	0.0532	0.0053	0.1218	0.0134	0.0174	0.0006	338.9	227.8	116.7	12.2	111.4	3.7
DL2014-85-14	210.8	269.9	0.78	0.0527	0.0109	0.1173	0.0211	0.0175	0.0010	322.3	405.5	112.6	19.2	112.2	6.6
DL2014-85-15	224.7	273.8	0.82	0.0528	0.0071	0.1139	0.0120	0.0167	0.0005	320.4	279.3	109.6	10.9	106.5	2.9
DL2014-85-16	215.3	219.6	0.98	0.0510	0.0083	0.1191	0.0166	0.0179	0.0009	239.0	350.0	114.2	15.1	114.2	5.9
DL2014-85-17	201.6	282.7	0.71	0.0540	0.0054	0.1184	0.0100	0.0169	0.0005	372.3	230.5	113.6	9.1	107.9	3.2
DL2014-85-19	261.4	248.7	1.05	0.0562	0.0137	0.1318	0.0257	0.0184	0.0017	457.5	468.2	125.7	23.0	117.6	10.7
DL2014-85-20	398.1	354.5	1.12	0.0506	0.0070	0.1177	0.0180	0.0168	0.0008	233.4	283.3	113.0	16.3	107.2	5.0
DL2014-85-21	235.5	228.2	1.03	0.0497	0.0074	0.1184	0.0196	0.0177	0.0014	189.0	305.5	113.6	17.8	113.4	9.2

量变化区间为 60.89%~72.00%，平均 69.39%，属于中酸性岩类； Al_2O_3 含量为 14.56%~16.00%，平均 14.97%； K_2O 含量为 3.08%~5.53%，平均 4.89%； Na_2O 含量为 3.13%~3.43%，平均 3.37%；全碱 $\text{K}_2\text{O}+\text{Na}_2\text{O}$ 为 6.88~8.96，平均值为 8.26； $\text{K}_2\text{O}/\text{Na}_2\text{O}$ 为 0.81~1.65，平均值为 1.47。火山岩的 MgO 、 CaO 、 TFe_2O_3 和 TiO_2 含量分别为 0.282%~2.39%、0.434%~4.27%、1.79%~6.11% 和 0.383%~0.872%，里特曼指数 $\delta=2.34\sim2.85$ ，其中流纹岩的 MgO 、 CaO 及 TFe_2O_3 含量极低，可能为后期蚀变流失。将样品投入岩浆分类图解 TAS 图解中，样品落入流纹岩及粗面安山岩范围；在 $\text{SiO}-\text{K}_2\text{O}$ 图解(图 4b)中，属于高钾钙碱性

及钾玄岩系列岩石；铝饱和指数(A/CNK)=0.92~1.28，在 A/CNK-A/NK 图解(图 4c)中落入准铝质和过铝质区域，在 $\text{Na}_2\text{O}-\text{K}_2\text{O}$ 关系图中落入(超)钾质岩石区域(图略)，在 $\text{ALK}-\text{MgO}-\text{TFeO}$ 图解中，样品投点均位于钙碱性系列(图 4d)。

美日切错组流纹岩及安山岩稀土元素分配曲线呈右倾平缓型(图 5a)，稀土总量(ΣREE)在 $141.52\times 10^{-6}\sim 236.05\times 10^{-6}$ 之间，轻稀土与重稀土总量(ΣLREE 与 ΣHREE)分别为 $126.69\times 10^{-6}\sim 212.94\times 10^{-6}$ 和 $14.83\times 10^{-6}\sim 23.11\times 10^{-6}$ ，轻稀土与重稀土比值(LREE/HREE)为 8.82~9.30；其中安山岩的轻稀土与重稀土总量(ΣLREE 与 ΣHREE)均比流纹岩低(表 2)。美日切错组火山岩

表2 西藏班怒带美日切错组火山岩的全岩主量元素(%)、微量元素($\times 10^{-6}$)分析结果Table 2 Whole-rock major(%), trace($\times 10^{-6}$) element data of the volcanic rocks from the Meiriqiecuo Fomation in the Bangonghu-Nujiang suture zone, Tibet

岩性	流纹岩				安山岩	岩性	流纹岩				安山岩
	DL2014-73	DL2014-74	DL2014-75	DL2014-76			样品号	DL2014-73	DL2014-74	DL2014-75	DL2014-76
SiO ₂	71.29	71.99	72	70.8	60.89	Sb	0.799	1.01	0.957	0.795	0.135
Al ₂ O ₃	14.73	14.88	14.7	14.56	16	Cs	7.19	9.44	7.66	8.9	3.78
TFe ₂ O ₃	1.81	1.79	1.84	1.98	6.11	Ba	710	803	743	716	518
MgO	0.282	0.287	0.309	0.309	2.39	La	47.6	53.9	50.2	46.2	30.8
CaO	0.447	0.437	0.434	0.594	4.27	Ce	80.6	96.6	88.8	82.6	57.2
Na ₂ O	3.34	3.16	3.13	3.43	3.8	Pr	10.2	11.1	10.7	9.63	6.54
K ₂ O	5.48	5.21	5.14	5.53	3.08	Nd	36.5	42.7	39.5	36.5	26.3
MnO ₂	0.024	0.024	0.04	0.049	0.097	Sm	6.43	7.15	6.57	6.13	4.66
TiO ₂	0.389	0.383	0.389	0.394	0.872	Eu	1.36	1.49	1.33	1.31	1.19
P ₂ O ₅	0.087	0.087	0.097	0.095	0.227	Gd	5.88	6.29	5.78	5.23	4.28
LOL	1.79	1.71	1.85	2.04	2.22	Tb	1.03	1.13	1.01	0.989	0.751
总量	99.67	99.96	99.93	99.78	99.96	Dy	5.4	6.08	5.68	5.28	3.99
A/CNK	1.20	1.28	1.28	1.15	0.92	Ho	1.1	1.18	1.09	1.01	0.759
A/NK	1.29	1.37	1.37	1.25	1.67	Er	3.14	3.59	3.4	3.05	2.24
K ₂ O+Na ₂ O	8.82	8.37	8.27	8.96	6.88	Tm	0.532	0.552	0.542	0.476	0.33
K ₂ O/Na ₂ O	1.64	1.65	1.64	1.61	0.81	Yb	3.09	3.71	3.35	3.11	2.16
δ	2.72	2.40	2.34	2.85	2.56	Lu	0.549	0.579	0.533	0.463	0.32
Li	83.2	121	55.8	99.9	43.4	W	1.75	1.73	1.58	1.45	1.2
Be	1.93	2.62	1.73	2.12	1.54	Tl	0.744	0.947	0.917	0.752	0.439
Sc	4.76	5.63	5.57	4.65	11.7	Pb	11.4	13.9	9.5	12	18.4
V	9.87	12.8	14.8	10.7	92.8	Bi	0.106	0.166	0.125	0.08	0.122
Cr	1.92	2.42	2.84	10.5	9.3	Th	16.9	19.8	18.2	16.1	10
Co	0.873	1.34	1.5	1.58	16.7	U	3.34	3.89	3.16	3.23	2.01
Ni	2.05	2.68	3.51	4.24	16.1	Nb	18.5	21.2	19.7	17.6	11.4
Cu	12	4.85	5.42	5.63	14.7	Ta	1.31	1.57	1.45	1.28	0.849
Zn	28.7	37	36.6	33.5	91.8	Zr	259	289	302	258	151
Ga	15.9	18.8	17.1	15.8	16.5	Hf	6.6	7.4	7.72	6.54	3.83
Rb	166	200	191	165	110	Σ REE	203.41	236.05	218.49	201.98	141.52
Sr	113	136	133	112	322	LREE	182.69	212.94	197.10	182.37	126.69
Y	29.9	33.5	30.7	28.6	22.1	HREE	20.72	23.11	21.39	19.61	14.83
Mo	0.916	0.906	0.717	1.64	0.893	LREE/HREE	8.82	9.21	9.22	9.30	8.54
Cd	0.326	0.372	0.383	0.365	0.288	La _N /Yb _N	11.05	10.42	10.75	10.66	10.23
In	0.045	0.045	0.042	0.04	0.049	δ Eu	0.66	0.66	0.65	0.69	0.80

注: A/CNK=Al₂O₃/(CaO+Na₂O+K₂O), A/NK=Al₂O₃/(Na₂O+K₂O), 里特曼指数(δ)=(Na₂O+K₂O)²/(SiO₂-43)

富集轻稀土, 亏损重稀土, La_N/Yb_N为10.42~11.05, 具轻重稀土分异明显的特征。火山岩 δ Eu为0.65~0.80, 具有中等负铕异常, 暗示原始岩浆经历了斜长石的分离结晶作用, 且其La_N/Sm_N为4.27~4.93, 暗示轻稀土之间发生了分馏; 而Gd_N/Yb_N为1.39~1.64, 暗示重稀土之间分馏不明显; δ Ce为0.85~0.94, 显示弱负铈异常, 暗示岩浆源区可能受到来自俯冲板片沉积物熔体的交代。在原始地幔标准化的微量元素蛛网图中(图5b)显示, 美日切错组火山岩富集Rb、K、Th、U、Pb等大离子亲石元素(LILE)和轻稀土元素(LREE), 相对亏损Nb、Ta、P、Ti等高场强元素(HFSE)和重稀土总量(HREE)的特征。另外, 美日切错组火山岩具有较

高的Sr($112 \times 10^{-6} \sim 322 \times 10^{-6}$)、较低的Y($22.1 \times 10^{-6} \sim 33.5 \times 10^{-6}$)、Yb($2.16 \times 10^{-6} \sim 3.71 \times 10^{-6}$), 以及较低Cr($1.92 \times 10^{-6} \sim 10.5 \times 10^{-6}$)、Ni($2.05 \times 10^{-6} \sim 16.1 \times 10^{-6}$)等相容元素含量。

3.3 Sr-Nd同位素组成

美日切错组中酸性火山岩Sr-Nd同位素组成见表3。中酸性火山岩⁸⁷Rb/⁸⁶Sr为0.9876~4.2516, ⁸⁷Sr/⁸⁶Sr为0.706860~0.711755, ¹⁴³Sm/¹⁴⁴Nd比值为0.1008~0.1067, ¹⁴³Nd/¹⁴⁴Nd比值为0.512497~0.512639, 具有高Sr低Nd的特征(表3)。根据上文所测火山岩锆石U-Pb加权平均年龄进行计算, 其(⁸⁷Sr/⁸⁶Sr)_i值为0.7050~0.7053, (¹⁴³Nd/¹⁴⁴Nd)_i为0.5124~0.5126, $\varepsilon_{\text{Nd}}(t)$ 值为-1.51

表 3 西藏班怒带美日切错组中酸性火山岩 Sr、Nd 同位素组成

Table 3 Sr and Nd isotopic compositions of the volcanic rocks from the Meiriqiecu Fomation in the Bangonghu-Nujiang suture zone, Tibet

样品号	岩性	$^{87}\text{Rb}/^{86}\text{Sr}$	$^{87}\text{Sr}/^{86}\text{Sr}$	$^{147}\text{Sm}/^{144}\text{Nd}$	$^{143}\text{Nd}/^{144}\text{Nd}$	$(^{87}\text{Sr}/^{86}\text{Sr})_i$	$(^{143}\text{Nd}/^{144}\text{Nd})_i$	$\epsilon_{\text{Nd}}(t)$	$\epsilon_{\text{Sr}}(t)$	T_{DM}	$T_{2\text{DM}}$
			(2σ)		(2σ)					(Ma)	(Ma)
DL2014-73	流纹岩	4.2471	0.711615 ± 15	0.1060	0.512639 ± 8	0.705037	0.512564	1.29	9.37	725	802
DL2014-74	流纹岩	4.2516	0.711755 ± 15	0.1008	0.512630 ± 6	0.705170	0.512558	1.18	11.26	704	809
DL2014-85	安山岩	0.9876	0.706860 ± 18	0.1067	0.512497 ± 7	0.705345	0.512422	-1.51	13.73	931	1029

表 4 西藏班怒带美日切错组中酸性火山岩锆石 Lu-Hf 同位素组成

Table 4 Zircon Lu-Hf isotopic composition of the volcanic rocks from the Meiriqiecu Fomation in the Bangonghu-Nujiang suture zone, Tibet

点号	U-P 年龄/Ma	$^{176}\text{Hf}/^{177}\text{Hf}$	$^{176}\text{Yb}/^{177}\text{Hf}$	$^{176}\text{Lu}/^{177}\text{Hf}$	$\pm 2\sigma$	$(^{176}\text{Hf}/^{177}\text{Hf})$	$\epsilon_{\text{Hf}}(0)$	$\epsilon_{\text{Hf}}(t)$	$T_{\text{DM}}^{\text{C}}(\text{Ma})$	$T_{2\text{DM}}^{\text{C}}(\text{Ma})$	$f_{\text{Lu/Hf}}$
DL2014-73-02	107.7	0.283081	0.045111	0.001675	0.000008	0.283077	10.9	13.2	246	325	-0.95
DL2014-73-03	110.1	0.283096	0.027302	0.001003	0.000001	0.283094	11.4	13.8	221	287	-0.97
DL2014-73-04	112.8	0.283033	0.031657	0.001180	0.000003	0.283031	9.2	11.6	311	428	-0.96
DL2014-73-05	110.1	0.283088	0.027864	0.001041	0.000004	0.283085	11.2	13.5	232	305	-0.97
DL2014-73-06	105.2	0.283091	0.021873	0.000805	0.000001	0.283089	11.3	13.5	227	300	-0.98
DL2014-73-07	108.0	0.283084	0.031963	0.001171	0.000007	0.283082	11.0	13.3	238	314	-0.96
DL2014-73-10	98.2	0.283128	0.040030	0.001450	0.000003	0.283126	12.6	14.7	176	222	-0.96
DL2014-73-11	111.2	0.283101	0.042085	0.001570	0.000011	0.283098	11.6	14.0	216	276	-0.95
DL2014-73-13	119.8	0.283046	0.028966	0.001106	0.000007	0.283044	9.7	12.2	292	394	-0.97
DL2014-73-17	115.9	0.283126	0.033260	0.001274	0.000004	0.283123	12.5	15.0	179	216	-0.96
DL2014-73-18	106.8	0.283127	0.038393	0.001469	0.000003	0.283124	12.6	14.8	178	219	-0.96
DL2014-73-19	111.3	0.283100	0.034659	0.001291	0.000005	0.283097	11.6	13.9	216	278	-0.96
DL2014-73-20	114.2	0.283143	0.049343	0.001781	0.000005	0.283139	13.1	15.5	156	180	-0.95
DL2014-85-01	109.0	0.282850	0.017070	0.000676	0.000005	0.282849	2.8	5.1	564	843	-0.98
DL2014-85-02	105.6	0.282847	0.026952	0.001045	0.000004	0.282845	2.7	4.9	574	854	-0.97
DL2014-85-04	106.6	0.282831	0.014374	0.000550	0.000002	0.282830	2.1	4.4	590	888	-0.98
DL2014-85-05	101.8	0.282858	0.017912	0.000697	0.000001	0.282857	3.0	5.2	554	830	-0.98
DL2014-85-07	110.6	0.282830	0.024478	0.000938	0.000007	0.282828	2.1	4.4	597	889	-0.97
DL2014-85-10	105.2	0.282830	0.019034	0.000744	0.000002	0.282829	2.1	4.3	594	891	-0.98
DL2014-85-11	111.4	0.282874	0.023894	0.000930	0.000004	0.282872	3.6	6.0	534	789	-0.97
DL2014-85-14	112.2	0.282929	0.030992	0.001225	0.000004	0.282926	5.5	7.9	461	666	-0.96
DL2014-85-15	106.5	0.282806	0.016956	0.000670	0.000001	0.282805	1.2	3.5	626	945	-0.98
DL2014-85-16	114.2	0.282845	0.020935	0.000824	0.000002	0.282843	2.6	5.0	575	854	-0.98
DL2014-85-17	107.9	0.282845	0.021774	0.000842	0.000001	0.282844	2.6	4.9	574	856	-0.97
DL2014-85-19	117.6	0.282823	0.020192	0.000802	0.000001	0.282821	1.8	4.3	605	900	-0.98
DL2014-85-20	107.2	0.282803	0.023989	0.000936	0.000005	0.282801	1.1	3.4	635	952	-0.97
DL2014-85-21	113.4	0.282800	0.026114	0.001013	0.000001	0.282798	1.0	3.4	641	956	-0.97

~ +1.29。其二阶模式年龄和一阶模式年龄值相似,一阶模式年龄值集中于 704~931 Ma,二阶模式年龄集中于 802~1029 Ma。将样品投入($^{87}\text{Sr}/^{86}\text{Sr}$)_i— $\epsilon_{\text{Nd}}(t)$ 四象限图中,落入第一、四象限(图 6)。

3.4 锆石 Lu-Hf 同位素

锆石的结晶温度和 Hf 同位素封闭温度较高,是目前示踪岩浆源区特征、反演源区物质时限的有效手段。本文对美日切错组火山岩锆石样品进行 MC-ICP-MS Lu-Hf 同位素测试。测试点位的选取基于已经进行过原位微区 U-Pb 同位素分析的单颗锆石。因此,Lu-Hf 同位素分析的测试点位少于 U-Pb 同位素分析点。美日切错组火山岩 27 个锆石

Lu-Hf 测点的 $^{176}\text{Yb}/^{177}\text{Hf}$ 值为 0.014374 ~ 0.049343,各点 $^{176}\text{Lu}/^{177}\text{Hf}$ 比值变化于 0.0008 ~ 0.0018 之间, $^{176}\text{Lu}/^{177}\text{Hf}$ 值均小于 0.002(表 4),说明锆石形成后的放射性成因 Hf 积累十分有限,因此,所测定的 $^{176}\text{Lu}/^{177}\text{Hf}$ 比值能较好地反映其形成过程中 Hf 同位素的组成特征(Patchett et al., 1981; Knudsen et al., 2001; Kinny et al., 2003; Wu FuYuan et al., 2007)。

流纹岩(DL2014-73)共计 13 个锆石测点的 $^{176}\text{Hf}/^{177}\text{Hf}$ 值分布于 0.283033 ~ 0.283143 之间,由对应的测点年龄计算得到初始 $^{176}\text{Hf}/^{177}\text{Hf}$ 比值为 0.283031 ~ 0.283139,Hf 同位素组成变化范围宽

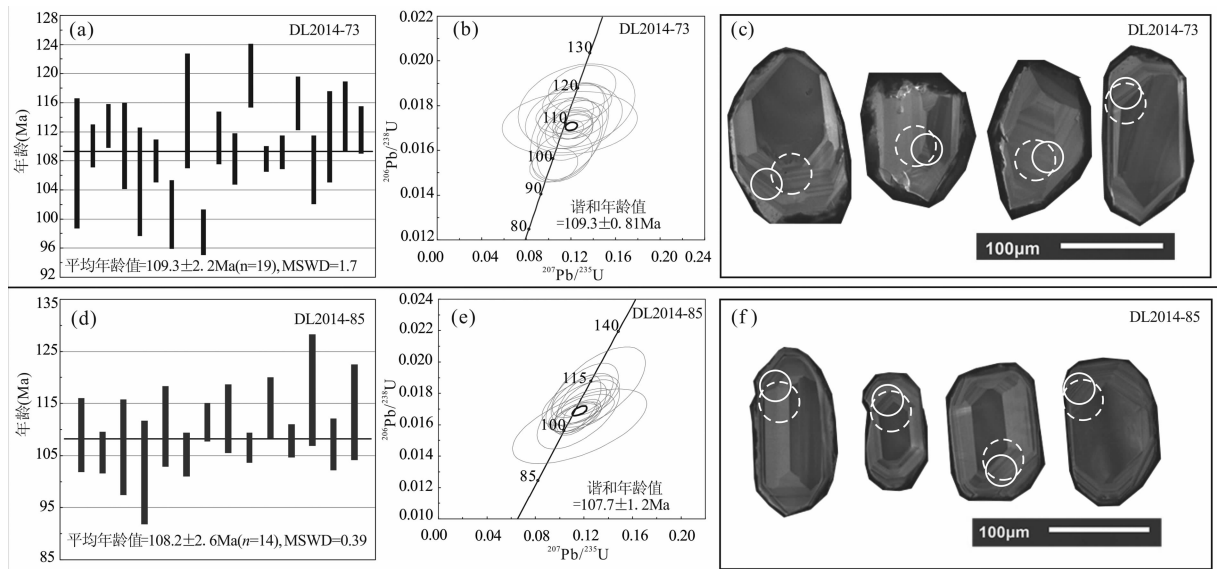


图 3 西藏班怒带美日切错组火山岩锆石 U-Pb 年龄谐和图和阴极发光图像

Fig. 3 Cathodoluminescence (CL) images and U-Pb Concordia diagrams of the volcanic rocks from the Meiriqiecuo Fomation in the Bangonghu-Nujiang suture zone, Tibet

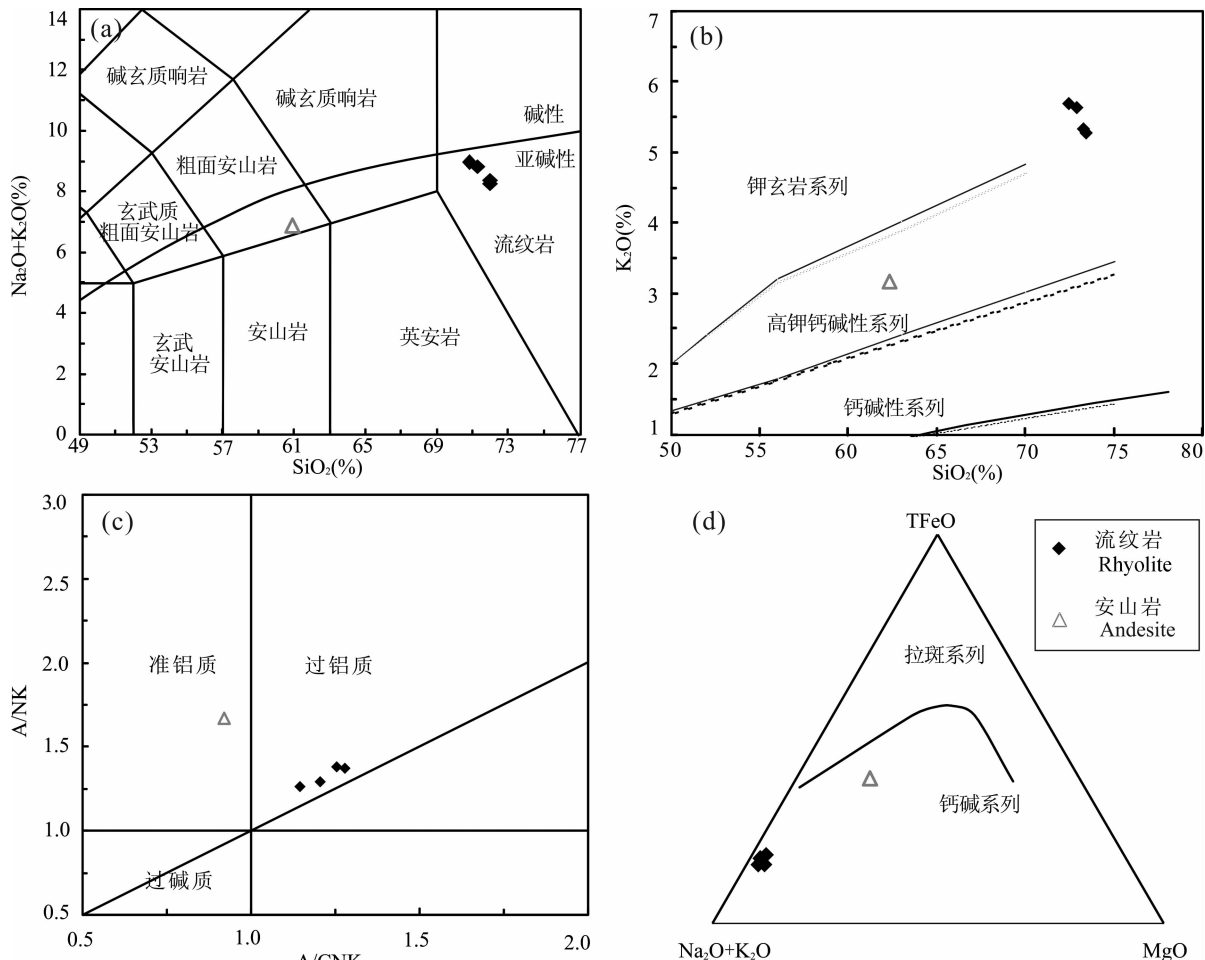
图 4 西藏班怒带美日切错组火山岩 TAS 图(据 Middlemost, 1994)、 $\text{SiO}_2-\text{K}_2\text{O}$ 图(据 Peccerillo et al., 1976)、 $\text{A}/\text{CNK}-\text{A}/\text{NK}$ 图(据 Maniar et al., 1989)和 ALK-MgO-TFeO 图解(据 Irvine et al., 1971)

Fig. 4 (a) Total alkalis vs. SiO_2 diagram (After Middlemost, 1994), (b) K_2O vs. SiO_2 diagram (After Peccerillo et al., 1976), (c) A/NK vs. A/CNK diagram (After Maniar et al., 1989), and (d) ALK-MgO-TFeO diagram (After Irvine et al., 1971) of the volcanic rocks from the Meiriqiecuo Fomation in the Bangonghu-Nujiang suture zone, Tibet

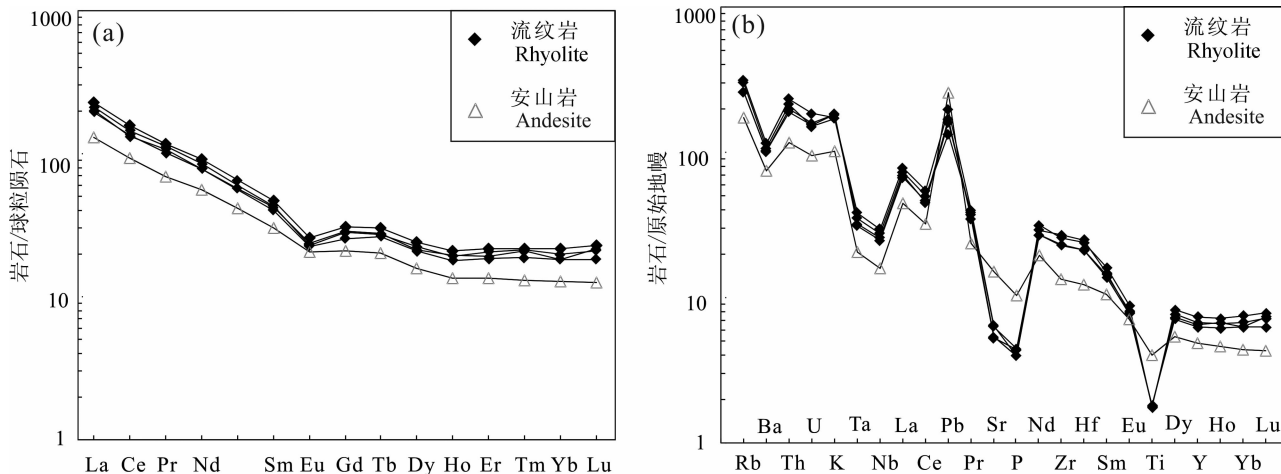


图 5 西藏班怒带美日切错组火山岩稀土元素球粒陨石标准化(a)和微量元素原始地幔标准化配分图(b); 标准化值据 Sun et al. (1989)

Fig. 5 Plots of chondrite-normalized REE(a) and primitive mantle-normalized trace elements(b) for the volcanic rocks from the Meiriqiecu Fomation in the Bangonghu-Nujiang suture zone, Tibet (after Sun et al., 1989)

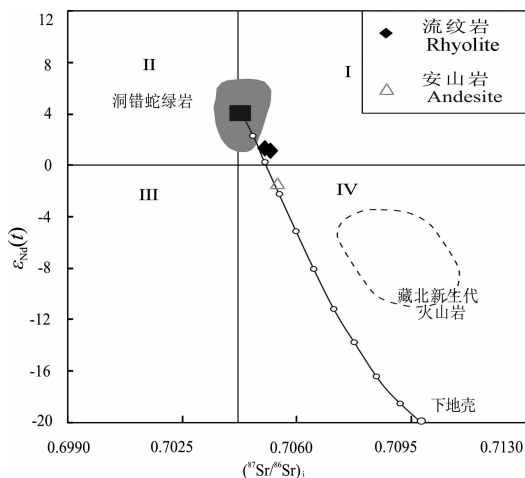


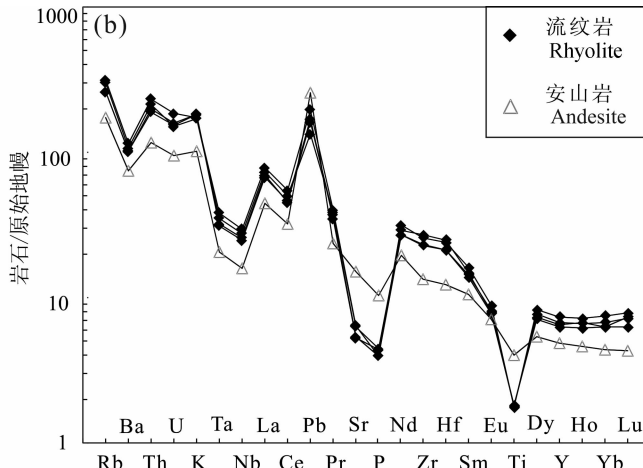
图 6 西藏班怒带美日切错组火山岩 Sr-Nd 图解
(据 Rollison, 2000)

Fig. 6 Sr-Nd diagrams of the volcanic rocks from the Meiriqiecu Fomation in the Bangonghu-Nujiang suture zone, Tibet (After Rollison, 2000)

藏北新生代火山岩据 Liu Shen et al., 2003, 洞错蛇绿岩据 Bao Peicheng et al., 2007, 下地壳据 Miller et al., 1999

Data sources: Cenozoic volcanic rocks in northern Tibet (Liu Shen et al., 2003), Dong-Co Ophiolite (Bao Peicheng et al., 2007), the lower crust (Miller et al., 1999)

泛, 对应的 $\epsilon_{\text{Hf}}(t)$ 为 $+11.6 \sim +15.5$, 平均值为 $+13.8$, 单阶段模式年龄 $T_{\text{DMC}} = 156 \sim 311 \text{ Ma}$, 平均值为 222.1 Ma , 两阶段模式年龄 $T_{\text{2DMC}} = 180 \sim 428 \text{ Ma}$, 平均值为 288.0 Ma 。安山岩(DL2014-85)共计 14 个锆石测点的 $^{176}\text{Hf}/^{177}\text{Hf}$ 值分布于 $0.282800 \sim 0.282929$ 之间, 由对应的测点年龄计算得到初始 $^{176}\text{Hf}/^{177}\text{Hf}$ 比值为 $0.282798 \sim 0.282926$,



Hf 同位素组成变化范围宽泛, 对应的 $\epsilon_{\text{Hf}}(t)$ 为 $+3.4 \sim +8.0$, 平均值为 $+4.8$, 单阶段模式年龄 $T_{\text{DMC}} = 461 \sim 641 \text{ Ma}$, 平均值为 548.1 Ma , 两阶段模式年龄 $T_{\text{2DMC}} = 666 \sim 956 \text{ Ma}$, 平均值为 813.1 Ma (图 7)。

4 讨论

4.1 火山岩成岩年龄

本文的火山岩样品采集自铁格隆南矿床及拿若矿床地表。野外勘查可见到美日切错组火山岩角度不整合地覆盖在曲色组($J_1 q$)和色哇组($J_{1-2} s$)地层之上(图 1), 这种构造—地层关系指示美日切错组火山岩代表了美日切错组火山作用的早期记录。由于美日切错组火山—沉积地层与上覆地层多数呈断层、角度不整合接触或被第四纪沉积物覆盖, 导致很难对美日切错组火山作用时代的上限进行约束。幸运的是, 本文获得美日切错组安山岩成岩年龄为 $108.2 \pm 2.6 \text{ Ma}$, 流纹岩成岩年龄为 $109.3 \pm 2.2 \text{ Ma}$, 两者在误差范围内相一致, 暗示美日切错组火山活动大约集中于 $108 \sim 109 \text{ Ma}$ 。美日切错组火山岩与热那错火山岩($109 \sim 111 \text{ Ma}$) (Chang Qingsong et al., 2011; Kapp et al., 2005) 成岩年龄相当, 表明班怒带北侧在 $108 \sim 111 \text{ Ma}$ 时发生了同时期的带状火山作用。前人在拉萨地块北部发现了大量 110 Ma 左右的火山活动记录, 包括巴尔达安山岩 (Zhang Liangliang et al., 2010), 巴尔错安山岩 (Chen Yue et al., 2010), 盐湖南部双峰式火山岩 (Sui et al., 2013), 那曲安山岩 (Huang Yu et al., 2012), 措勤地区则弄群火山岩及大面积出露的多尼

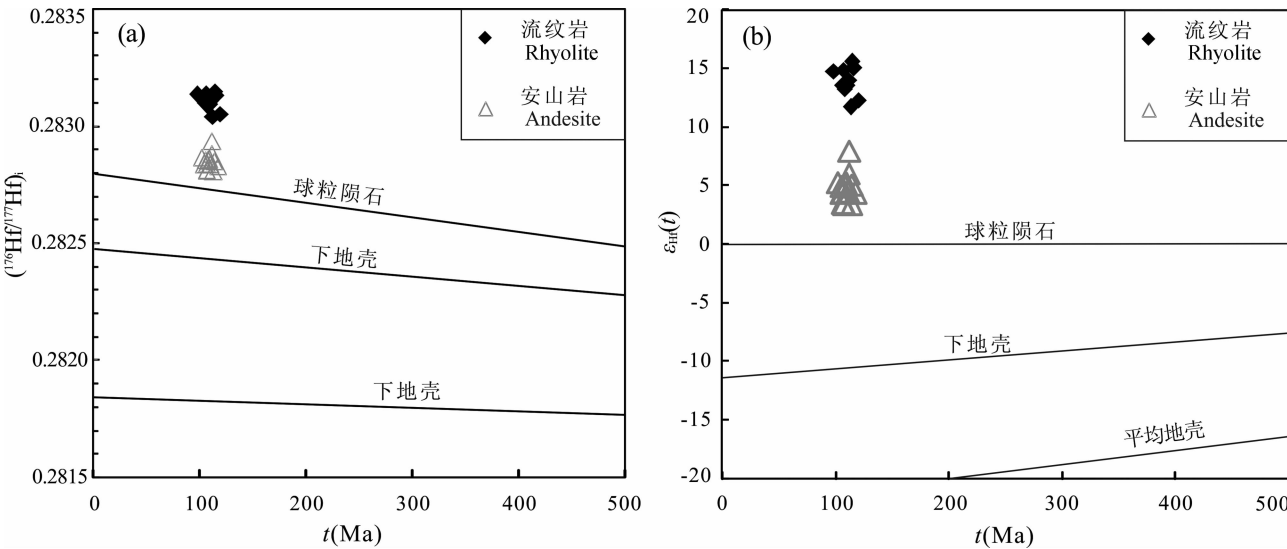
图7 西藏班怒带美日切错组火山岩的 $^{176}\text{Hf}/^{177}\text{Hf}$ - t 和 $\epsilon_{\text{Hf}}(t)$ - t 图解

Fig. 7 Diagram of $\epsilon_{\text{Hf}}(t)$ vs. t and $^{176}\text{Hf}/^{177}\text{Hf}$ vs. t of the volcanic rocks from the Meiriqiecuo Fomation in the Bangonghu-Nujiang suture zone, Tibet

组、去申拉组火山岩等(Zhu Dichen et al., 2008a, 2008b)。这些新的高质量年代学数据很可能暗示,早白垩世 110 Ma 左右时,班公湖—怒江缝合带南北两侧发生了同时期的带状火山喷发作用。

4.2 岩石成因与源区性质探讨

美日切错组火山岩富集大离子亲石元素(LILE)和轻稀土元素(LREE),而亏损高场元素(HFSE:Nb、Ta、Zr、Ti)和重稀土元素(HREE)(图 5a,b),低的 TiO_2 (<1%) 含量,具有岛弧岩浆的独特的地球化学特征。 $(\text{La/Yb})_N$ 为 10.23~11.05, Sr/Y 比值介于 3.78~14.57 之间;在 Sr/Y -Y 图解和 La_N/Yb_N -Yb_N 图解落入经典岛弧岩石系列(图略)。美日切错组火山岩 $\text{K}_2\text{O}/\text{Na}_2\text{O}$ 为 0.81~1.65,属于钾质—超钾质岩。已有研究表明,产出钾质—超钾质火山岩构造环境通常有五种类型:板块内部(WIP)、大陆弧(CAP)、后碰撞弧(PAP)、早期洋弧(IOP)和晚期洋弧(LOP)(Morrison, 1980; Müllker et al., 1992)。将火山岩样品点投影到 Müllker et al. (1992) 的构造判别图解中进行判别(图 8)。在 $\text{TiO}_2/100$ -La-Hf×10 图解中(8a),本区火山岩投点均落于陆缘弧火山岩环境中;在 $\text{Zr} \times 3$ -Nb×50-Ce/ P_2O_5 图解中(图 8b),样品点均投于大陆弧区域。Yb 为不活动元素,其行为类似于不相容元素。因此,在部分熔融和分离结晶作用过程中,Th/Yb 比值将保持不变,Ta/Yb 比值与此类似(Pearce, 1983)。Bailey (1981) 认为 La/Yb 比值可以作为度量岛弧安山质岩浆生成过程中大陆地壳参与的程度。

度,并利用 La/Yb-Sc/Ni 图解识别出低钾大洋岛弧安山岩、其它大洋岛弧安山岩、大陆岛弧安山岩和安第斯型(活动大陆边缘)安山岩等四种类型(图 8c),将样品投入该图解中,样品落入安第斯型(活动大陆边缘)安山岩。在 Th/Yb-Ta/Yb 构造判别图解上(图 8d),火山岩样品均位于活动大陆边缘范围内。说明美日切错组火山岩为俯冲阶段岩浆作用产物,形成于班公湖—怒江中特斯洋壳向北的俯冲阶段。

本文火山岩 $^{87}\text{Sr}/^{86}\text{Sr}$ 比值为 0.706860~0.711755,高于原始地幔现代 $^{87}\text{Sr}/^{86}\text{Sr}$ 比值(0.7045)(DePaolo et al., 1979); $^{143}\text{Nd}/^{144}\text{Nd}$ 比值为 0.512497~0.512639,低于原始地幔现代 $^{143}\text{Nd}/^{144}\text{Nd}$ 比值(0.51264)(Jacobson et al., 1980);其 $(^{87}\text{Sr}/^{86}\text{Sr})_i$ 值为 0.7050~0.7053, $(^{143}\text{Nd}/^{144}\text{Nd})_i$ 为 0.5124~0.5126, $\epsilon_{\text{Nd}}(t)$ 值为 -1.51~+1.29,表现出高 Sr、低 Nd 及低 ϵ_{Nd} 值的特征,通常火山岩的这些特征或者与俯冲作用改造的岩石圈富集地幔有关(Tarney et al., 1994),或者与岩浆上侵过程中地壳混染有关(Ma et al., 1998)。将样品投入 $(^{87}\text{Sr}/^{86}\text{Sr})_i-\epsilon_{\text{Nd}}(t)$ 四象限图解中,落点分布于俯冲洋壳岩石圈板片熔融形成的玄武岩与下地壳混合线附近,明显反映出其源岩的初生洋壳属性。岩石稀土总量较低(141.52×10^{-6} ~ 236.05×10^{-6}), δEu 为 0.65~0.80,球粒陨石标准化配分曲线为 Eu 异常不明显的右倾型,轻稀土明显富集。岩石均为弱的负 δCe 异常、较小的 Ce/Pb 值(3.11~9.35),以及高 Sr 低 Nd 特征,暗示火山

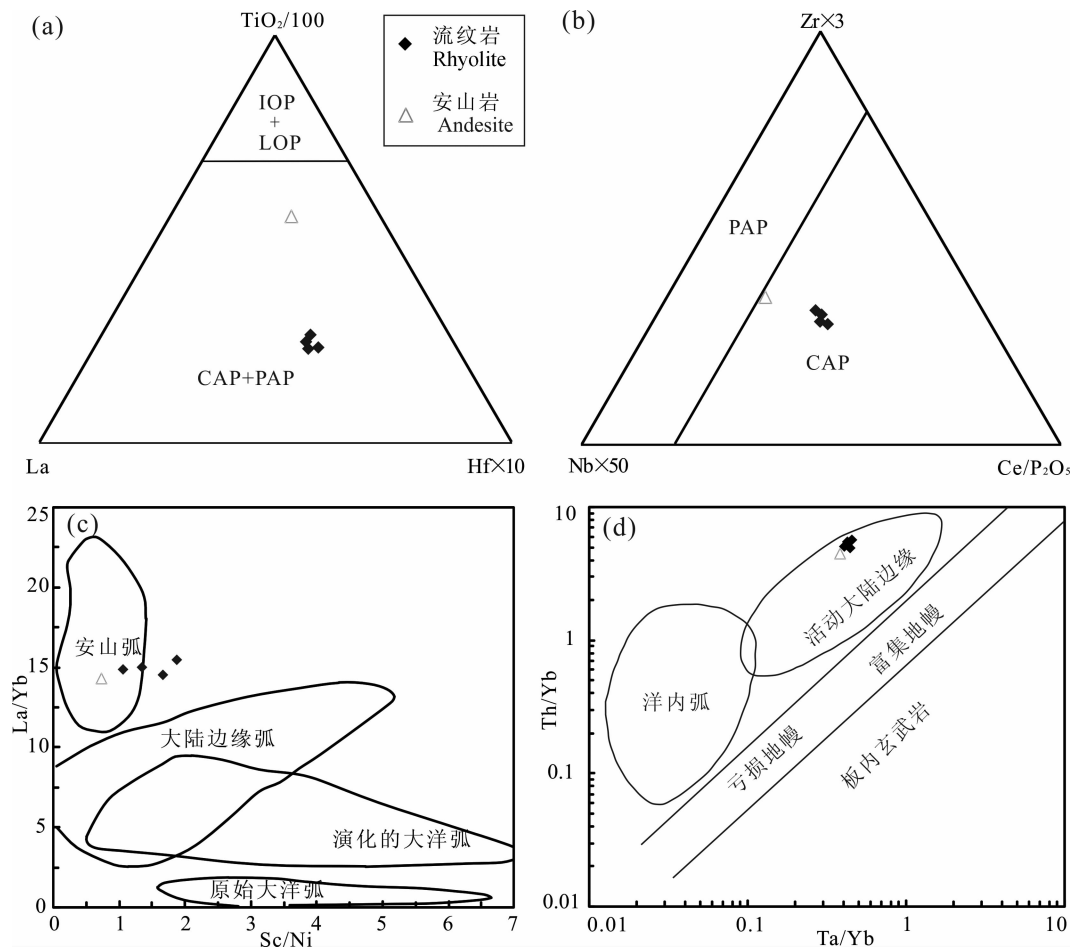


图 8 西藏班怒带美日切错组火山岩构造环境判别图(a图和b图据 Morrison, 1980;
c图据 Pearce, 1982; d图据 Condie et al., 1986)

Fig. 8 Discrimination diagrams of tectonic setting of the volcanic rocks from the Meiriqiecuo Formation in the Bangonghu-Nujiang suture zone, Tibet((a) and (b) after Morrison, 1980; (c) after Pearce, 1982; (d) after Condie et al., 1986)

岩形成过程中有俯冲沉积物的加入(Dong Guogong et al., 2008)。

美日切错组流纹岩 $\epsilon_{\text{Hf}}(t)$ 为 $+11.6 \sim +15.5$, 安山岩 $\epsilon_{\text{Hf}}(t)$ 为 $+3.4 \sim +7.9$, 存在较大的变化范围, 相对应的 $^{176}\text{Hf}/^{177}\text{Hf}$ 值变化也较大, 显示出锆石的 Hf 同位素具有不均一性, 可能为开放的体系引起熔体的这种变化(Kemp et al., 2007)。由于锆石 Hf 同位素体系具有很高的封闭温度(Patchett et al., 1983), 其 Hf 同位素体系不会随部分熔融或者分离结晶过程而出现变化, 因此可以推论锆石 Hf 同位素比值的不均一性应归因于更具放射性成因 Hf 的幔源和有着较少 Hf 同位素壳源这两种不同端元的相互作用(Bolhar et al., 2008)。 $\epsilon_{\text{Hf}}(t)$ 和 $^{176}\text{Hf}/^{177}\text{Hf}$ 值变化范围宽泛, 在 $\epsilon_{\text{Hf}}(t)$ - t 图解和 $(^{176}\text{Hf}/^{177}\text{Hf})_t$ - t 图解(图 7)中, 美日切错组火山岩投点均落在了球粒陨石之上, 暗示可能直接起源于亏损地幔橄榄岩部分熔融(Li et al., 2014b), 或是新生

下地壳部分熔融形成的酸性岩浆与持续底侵的幔源玄武质岩浆混合的产物(Ratajeski et al., 2005)。与下地壳部分熔融有关的岩浆产物 $Mg^{\#}$ 一般小于 40(Atherton et al., 1993), 而直接起源于亏损地幔楔橄榄岩部分熔融型形成的岩浆 $Mg^{\#}$ 大于 60(McCarron et al., 1998), 美日切错组火山岩具有较低的 $Mg^{\#}$ 值, 变化于 $23.76 \sim 43.90$ (平均值 28.18), 反映其岩浆并非直接起源于地幔楔橄榄岩的部分熔融, 更有可能是新生下地壳部分熔融形成的酸性岩浆与幔源玄武质岩浆混合的结果。实验岩石学表明, 玄武质岩石部分熔融形成的中酸性熔体具有低的 Cr、Ni 含量及较低的 $Mg^{\#}(<45)$, 而加入 10% 橄榄岩可使 $Mg^{\#}$ 增高, 并导致 Cr、Ni 等相容元素含量增加(Noll et al., 1996)。美日切错组安山岩具有比流纹岩相对较高的 Cr、Ni 和 $Mg^{\#}$, 可能暗示流纹岩的原始混合岩浆中下地壳玄武质岩石部分熔融形成的酸性岩浆占有较大比例, 安山岩的原始

混合岩浆中地幔橄榄岩组分参与部分熔融的比例相对较高。新生下地壳是由幔源物质部分熔融形成玄武质母岩浆后向上运移,滞留在壳幔边界形成,其往往继承了幔源源区的同位素特征(Ratajeski et al., 2005)。美日切错组火山岩适中的 $\text{La}_{\text{N}}/\text{Yb}_{\text{N}}$ (10.42~11.05),高的($^{87}\text{Sr}/^{86}\text{Sr}$)_i和不够高的($^{143}\text{Nd}/^{144}\text{Nd}$)、高的正 $\epsilon_{\text{Hf}}(t)$ 值及变化范围较大的 $\epsilon_{\text{Hf}}(t)$ 等特征,亦指示其可能为新生下地壳镁铁质岩石部分熔融所形成。

综上所述,本文认为美日切错组火山岩是处于班公湖—怒江中特斯洋壳向北的俯冲背景下,由俯冲板片脱水产生流体交代地幔楔发生部分熔融形成原始玄武质岩浆,并在上升后,滞留在壳幔边界形成新生下地壳,新生下地壳与持续底侵幔源玄武质岩浆混合而部分熔融形成。

4.3 地球动力学背景讨论

岩石地球化学特征研究显示,本区火山岩属于高钾钙碱性及钾玄岩系列,与传统的以低钾、中钾钙碱性火山岩为主的岛弧火山岩(Deng Jinfu et al., 2007)和典型的后碰撞钙碱性火山岩(Mo Xuanxue et al., 2001)不符,而与秘鲁南部和智利北部的中安第斯火山岩($16^{\circ} \sim 26^{\circ}$ S)具有很强的相似性(Ramos, 1999),且样品的 La/Yb 比值均大于2,显示出活动大陆边缘火山岩的性质(Wu Genyao et al., 1999)。意味着多龙矿集区早白垩世($108 \sim 109$ Ma)岩浆活动主要发生于厚地壳背景下与板片俯冲有关的岛弧环境,很可能如中安第斯($16^{\circ} \sim 26^{\circ}$ S)一样俯冲板片的角度变陡(Ramos, 1999; Coira et al., 1994)。因为由于低角度或平板俯冲要么形成隔热层不能产生岛弧岩浆(因不存在交代的软流圈地幔楔),要么在俯冲板片的前缘形成埃达克岩(Gutscher et al., 2000)。然而本文报道的美日切错组火山岩高质量的锆石U-Pb年代学及地球化学证据,以及本区中酸性侵入岩相关数据(Chen Huaan et al., 2013; Fang Xiang et al., 2015; Li Jinxiang et al., 2008; Li et al., 2011b, 2013 and 2014a; Qu Xiaoming et al., 2006; She Hongquan et al., 2009; Zhu Xiangping et al., 2015),暗示了早白垩世时本区存在被俯冲板片流体交代的软流圈地幔楔。因此可以排除班公湖—怒江特提斯洋壳以低角度或平板俯冲模式来解释多龙矿集区白垩纪岩浆作用的地球动力学背景的可能。

对于班公湖—怒江洋盆俯冲的极性,不同学者提出了向北俯冲(Ding et al., 2003a, 2003b;

Girardeau et al., 1984; Guynn et al., 2006; Matte et al., 1996; Pearce et al., 1988; Zhang et al., 2004)、向南俯冲(Bao Peicheng et al., 2007; Hsu et al., 1995; Zhu Dicheng et al., 2006a, 2006b, 2008a and 2008b)以及双向俯冲(Mo Xuanxue et al., 2001; Pan Guitang et al., 2004)的不同认识。依据本区火山岩地球化学特征可知,其具有典型岛弧岩浆性质。从空间分布上看(图1),多龙矿集区位于青藏高原腹地的狮泉河—改则—洞错蛇绿岩带北侧,区内火山岩及中酸性侵入岩形成于早白垩世,表明班公湖—怒江特提斯洋壳至少存在早白垩世向北俯冲的性质。研究表明,班公湖—怒江特提斯洋于三叠纪或早侏罗世开启(Qiu Ruizhao et al., 2004)。Shi(2007)对班公湖—怒江新特提斯蛇绿岩带SSZ型蛇绿岩中的辉长岩进行锆石SHRIMP U-Pb定年得到 167.0 ± 1.4 Ma,代表了新特提斯洋在该区俯冲消减的时限,指示班公湖—怒江新特提斯洋至少从中侏罗世开始由扩张转换为俯冲消减;Kapp et al.(2005, 2007)根据狮泉河蛇绿岩、区域构造和缝合带沉积相分析,指出班公湖—怒江洋盆早侏罗世扩张成深海洋盆,晚侏罗世洋壳开始向北侧羌塘地块之下俯冲消减,至侏罗纪末—白垩纪初洋盆闭合,此后进入弧—陆碰撞演化阶段。Guo Tieying et al.(1991)根据不整合于蛇绿岩上的上侏罗统地层研究,认为班公湖地区新特提斯洋于早白垩世关闭。然而,新近研究发现多龙矿集区内广泛发育形成于典型的岛弧构造背景下的约120 Ma的含矿花岗闪长斑岩;Zhu Dicheng et al.(2006a, 2006b)发现双湖南部仁木地区大面积发育约110 Ma的洋岛玄武岩,指示班公湖—怒江洋盆的关闭时间明显晚于晚侏罗世—早白垩世早期。本文获得本区安山岩成岩年龄为 108.2 ± 2.6 Ma,流纹岩成岩年龄为 109.3 ± 2.2 Ma,暗示班公湖—怒江特提斯洋壳于早白垩世晚期($108 \sim 109$ Ma)尚未关闭,仍在向北俯冲于羌塘地块之下,拉萨地块与羌塘地块碰撞时间应晚于早白垩世晚期。

Zhu et al.(2009, 2011)主张在早白垩世早期,随着班公湖—怒江特提斯板片的脱水熔融而形成了一系列的岛弧火山岩。大约在 113 ± 5 Ma,班公湖—怒江特提斯洋壳出现了断离(break-off),使得软流圈上涌,烘烤了岩石圈地幔物质,乃至熔融,造成了 113 ± 5 Ma时期的岩浆大爆发。多龙矿集区美日切错组火山岩出露于班公湖—怒江缝合带北侧的羌塘地块南缘,锆石U-Pb年代学数据显示安山岩成

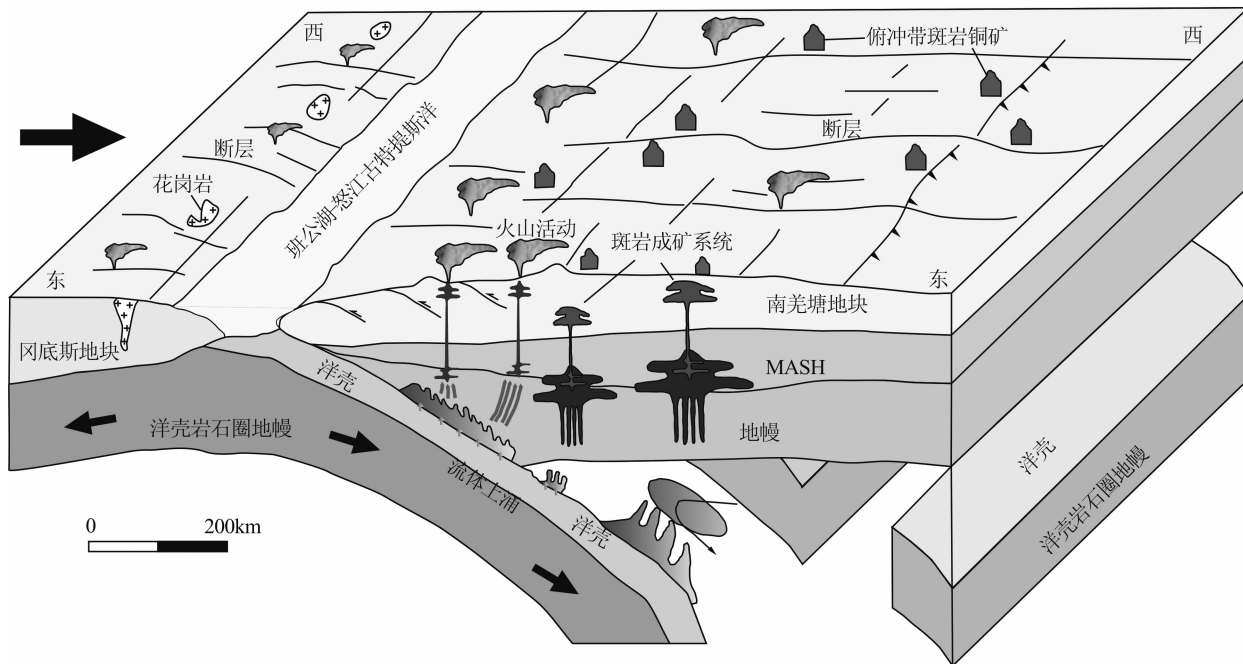


图 9 西藏多龙矿集区的成矿模式简图(据 Richards, 2003; Wilkinson, 2013)

Fig. 9 Suprasubduction zone setting for the formation of the Duolong deposit, Tibet(after Richards, 2003; Wilkinson, 2013)

岩年龄为 108.2 ± 2.6 Ma, 流纹岩成岩年龄为 109.3 ± 2.2 Ma, 与 113 ± 5 Ma 岩浆大爆发时间重合, 班怒带早白垩世 110 Ma 左右南北两侧明显发生了同时期带状岛弧型火山作用。故本文认为早白垩世早期(约 110 Ma), 班公湖—怒江特提斯洋壳发生双向俯冲(图 9), 洋壳出现了断离(break-off), 班怒缝合带南北侧发生大规模的同时期带状火山作用。

5 结论

(1) 美日切错组安山岩锆石 U-Pb 年龄为 108.2 ± 2.6 Ma, 流纹岩锆石 U-Pb 年龄为 109.3 ± 2.2 Ma, 矿集区火山活动集中于早白垩世晚期; 与冈底斯地块的大量早白垩世火山岩同期。

(2) 美日切错组火山岩属于高钾钙碱性岩石及钾玄岩系列岩石, 富集轻稀土(LREE)和大离子亲石元素(LILE), 亏损重稀土(HREE)及高场强元素(HFSE)。轻重稀土分异明显的特征, 轻稀土之间发生明显分馏, 重稀土之间分馏不明显, δEu 具有中等负异常, $(^{87}\text{Sr}/^{86}\text{Sr})_i$ 值为 $0.7050 \sim 0.7053$, $(^{143}\text{Nd}/^{144}\text{Nd})_i$ 为 $0.5124 \sim 0.5126$, $\epsilon_{\text{Nd}}(t)$ 值为 $-1.51 \sim -1.29$ 。流纹岩 $\epsilon_{\text{HF}}(t)$ 为 $+11.6 \sim +15.5$, 平均值为 $+13.8$, 两阶段模式年龄平均值为 288.0 Ma; 安山岩 $\epsilon_{\text{HF}}(t)$ 为 $+3.4 \sim +8.0$, 平均值为 $+4.8$, 两阶段模式年龄平均值为 813.1 Ma, 表现出明显的幔源特征。美日切错组火山岩是处于班公湖

—怒江新特提斯洋洋壳向北的俯冲背景下, 由俯冲板片脱水产生流体交代地幔楔发生部分熔融形成原始玄武质岩浆, 并在上升滞留在壳幔边界形成新生下地壳, 新生下地壳与持续底侵幔源玄武质岩浆混合而部分熔融形成。

(3) 美日切错组火山岩形成于典型岛弧的构造背景下, 暗示班公湖—怒江洋盆在早白垩世晚期($108 \sim 109$ Ma)正在向北俯冲于羌塘地块之下且俯冲板片的角度变陡, 尚未关闭, 拉萨地块与羌塘地块碰撞时间应晚于早白垩世晚期($108 \sim 109$ Ma)。

致谢: 感谢西藏地调院李玉彬工程师、西藏地勘局第五地质大队李彦波工程师在野外工作过程中给予的帮助。感谢中国地质大学(北京)董国臣教授及黄雄飞博士在室内研究及论文成文中的提供的建议和帮助, 以及匿名老师对稿件提出的修改意见。感谢中国地质科学院矿产资源研究所 LA-MC-ICP-MS 实验室、核工业北京地质研究院实验室、中国地质大学(北京)地质过程与矿产资源国家重点实验室以及西北大学大陆动力学国家重点实验室的老师在样品分析测试过程中提供大量帮助。

References

- Atherton M P, Petford N. 1993. Generation of sodium-rich magmas from newly underplated basaltic crust. *Nature*, 362:144~146.
Bailey J C. 1981. Geochemical criteria for a refined tectonic discrimination of orogenic andesites. *Chemical Geology*, 32:

- 139~154.
- Bao Peicheng, Xiao Xuchang, Su li, Wang Jun. 2007. Geochemical characteristics and isotopic dating for the Dongcuo Ophiolite, Tibet Platea. *Science in China: Series D: Earth Sciences*, 37 (3):298~307. (in Chinese with English abstract).
- Bolhar R, Weaver S D, Whitehouse M J, Palin J M, Woodhead J D, Cole J W, 2008. Sources and evolution of arc magmas inferred from coupled O and Hf isotope systematics of plutonic zircons from the Cretaceous Separation Point Suite (New Zealand). *Earth and Planetary Science Letters* 268, 312~324.
- Chang Qingsong, Zhu Dicheng, Zhao Zhidan, Dong Guochen, Mo Xuanxue, Liu Yongsheng and Hu Zhaochu 2011. Zircon U-Pb geochronology and Hf isotopes of the Early Cretaceous Rena-Co rhyolites from southern margin of Qiangtang, Tibet and their implications. *Acta Petrologica Sinica*, 27(7):2034~2044. (in Chinese with English abstract).
- Chen Huaan, Zhu Xiangping, Ma Dongfang, Huang Hanxiao, Li Guangming, Li Yubin, Li Yuchang, Wei LuJie, Liu Chaoqiang. 2013. Geochronology and Geochemistry of the bolong Porphyry Cu-Au deposit, Tibet and its mineralizing significance. *Acta Geologica Sinica*, 87(10):1~19. (in Chinese with English abstract).
- Chen Yue, Zhu Dicheng, Zhao Zhidan, Zhang Liangliang, Liu Ming, Yu Feng, Guan Qi, Mo Xuanxue. 2010. Geochronology, geochemistry and petrogenesis of the Bam co andesites from the northern gangdese. Tibet. *Acta Geologica Sinica*, 26 (7): 2193 ~ 2206. (in Chinese with English abstract).
- Coira B, Mahlburg Kay S and Viramonte J. 1994. Upper Cenozoic magmatic evolution of the Argentine Puna: A model for changing subduction geometry. *International Geology Review*, 35:677~720.
- Condie K C, Bowring G P, Allen P. 1986. Origin of granitesinan Archean high grade terrane, southern India. *Contributions to Mineralogy and Petrology*, 92(1): 93~103.
- Cui Ning, Xing Shuwen, Xiao Keyan, Ding Jianhua. 2016. Geological characteristics and resource potential analysis of the Bangong Nujiang Cu-Au-Fe-Li metallogenic belt. *Acta Geologica Sinica*, 90(7):1623~1635.
- Deng Jinfu, Xiao Qinghui, Su Shangguo, Liu Cui, Zhao Guochun, Wu Zong-xu, Liu Yong. 2007. Igneous Petrotectonic Assemblages and Tectonic Settings: A Discussion. *Geological Journal of China Universities*. 13 (3) 392 ~ 402. (in Chinese with English abstract).
- DePaolo D J and Wasserburg G J. 1979. Inferences about magma sources and mantle structure from variations of $^{143}\text{Nd} / ^{144}\text{Nd}$. *Geophysical Research Letters*,3(12):743~746.
- Ding L, Kapp P, Yin A, Wang M D. 2003a. Early Tertiary volcanism in the Qiangtang terrane of central Tibet: evidence for a transition from oceanic to continental subduction. *Journal of Petralogy*,44:1833~1865.
- Ding L and Lai Q Z. 2003b. New geological evidence of crustal thickening in the Gangdese block prior to the Indo-Asian collision. *Chinese Science Bulletin*, 48(15):1604~1610.
- Dong Guogong, Mo Xuanxue, Zhao Zhidan, Zhu Dicheng, Song Yuntao, Wang Lei. 2008. Gabbros from southern gangdese: implication for mass exchange between mantle and crust. *Acta Geologica Sinica*, 24 (2):203 ~ 210. (in Chinese with English abstract).
- Duan Zhi-ming, Li Guangming, Zhang Hui, Duan Yaoyao. 2013. The formation and its geologic significance of late Triassic-Jurassic accretionary complexes and constraints on metallogenic and geological setting in Duolong porphyry copper gold ore concentration area, northern Bangong Co-Nujiang suture zone, Tibet. *Geological Bulletin of China*, 32 (5): 742 ~ 750. (in Chinese with English abstract).
- Fang Xiang, Tang Juxing, Song Yang, Yang Chao, Ding Shuai, Wang Yi-yun, Wang Qin, Sun Xingguo, Li Yubin, Wei Lu-jie, Zhang Zhi, Yang Huanhuan Gao Ke, Tang Pan. 2015. Formation Epoch of the South Tiegelong Supelarge Epothermal Cu (Au-Ag) Deposit in Tibet and Its Geological Implications. *Acta Geoscientifica Sinica*. 36 (2):168~176. (in Chinese with English abstract).
- Girardeau J, Marcoux J, Allegre C J, Bassoulet J P, Tang Y K, Xiao X C, Zao Y G, Wang X B. 1984. Tectonic environment and geodynamic significance of the Neo-Cimmerian Donqiao Ophiolite, Bangong-Nujiang suture zone, Tibet. *Nature* 307: 27~31.
- Guo Tieying, Liang Dingyi, Zhang Yizhi. 1991. geologyof Ali, Tibet. *Wuhan: China University of Geosciences*, 1~106.
- Gutscher M A, Maury R and Eissen J P. 2000. Can slab melting be caused by flat subduction? *Geology*, 28(6):535~538
- Guynn J H, Kapp P, Pullen A, Heizler M; Gehrels G; Ding L. 2006. Tibetan basement rocks near Amdo reveal “missing” Mesozoic tectonism along the Bangong suture, central Tibet. *Geology* 34, 505~508.
- Hanchar J M, Miller C F. 1993. Zircon zonation patterns as revealed by cathodoluminescence and backscattered electron images: Implications for interpretation of complex crustal histories. *Chemical Geology*,110(1~3):1~13.
- Hou KeJun, Li YanHe and Tian YouRong. 2009. In situ U-Pb zircon dating using laser ablation-multi ion counting-ICP-MS. *Mineral deposits*, 28(4):481~492. (in Chinese with English abstract).
- Hsu K J. Pan G T, Sengor A M C. 1995, Tectonic evolution of the Tibetan plateau:a working hypothesis based on the archipelago model of orogenesis. *International Geology Review*, 37: 473 ~508.
- Huang Yu, Zhu Dicheng, Zhao Zhidan, Zhang Liangliang, Don Depalolo, Hu Zhaochu, Yuan Honglin, Mo Xuanxue. 2012. Petrogenesis and implication of the andesites at ~113Ma in the Nagqu region in the northern Lhasa subterrane. *Acta Geologica Sinica*,28(5):1603~1614. (in Chinese with English abstract).
- Irvine T N and Baragar W R A. 1971. A guide to the chemical

- classification of the common volcanic rocks. Canadian Journal of Earth Sciences, 8:523~548.
- Jacobson SB and Wasserburg GJ. 1980. Sm-Nd isotopic evolution of chondrites. Earth and Planetary Science Letters, 50(1): 139~155.
- Kapp P, Murphy M A, Yin A, Harrison TM, Ding L, Guo JH. 2003. Mesozoic and Cenozoic tectonic evolution of the Shiquanhe district of western Tibet. Tectonics, 22(4): 3~23.
- Kapp P, Yin A, Harrison T M, Ding L., 2005. Cretaceous-Tertiary shortening, basin development, and volcanism in central Tibet. Geological Society of America Bulletin, 117: 865~878.
- Kapp P, DeCelles P G., Gehrels G E., Heizler M, Ding L, 2007. Geological records of the Lhasa-Qiangtang and Indo-Asian collisions in the Nima area of central Tibet. Geological Society of America Bulletin 119, 917~933.
- Kathmandu. 1986. Philosophical Transactions of the Royal Society A327, 215~238.
- Kemp A I, Hawkesworth CJ, Foster G L, Paterson B A, Woodhead J D, Herdt J M, Gray C M, Whitehouse M J. 2007. Magmatic and crustal differentiation history of granitic rocks from Hf-O isotopes in zircon. Science, 315: 980~983.
- Kinny P D, Mass R. 2003. Lu-Hf and Sm-Nd isotope systems in zircon. In: Hachar JM and Hoskin PWO(eds.) Zircon. Rev. Mineral. Geochem, 53:327~341.
- Knudsen T L, Griffin, Hartz E, Andresen A, Jackson S. 2001. In-situ hafnium and lead isotope analyses of detrital zircons from the Devonian sedimentary basin of NE Greenland: a record of repeated crustal reworking. Contributions to Mineralogy and Petrology, 141:83~94.
- Li Guangming, Li Jinxiang, Qin Kezhang, Zhang TianPing and Xiao Bo. 2007. High temperature, Salinity and strong oxidation ore-forming fluid at Duobuza Gold-rich porphyry copper deposit in the bangonghu tectonic belt, Tibet: Evidence from fluid inclusions. Acta Petrologica, 23(5): 935~952. (in Chinese with English abstract).
- Li Jinxiang, Li Guangming, Qin Kezhang, and Xiao Bo. 2008. Geochemistry Of porphyries and volcanic rocks and ore-forming geochronology of Duobuza gold-rich porphyry copper deposit in Bangonghu Belt, Tibet: Constraints on metallogenetic tectonic settings. Acta Petrologica, 24(3):531~543. (in Chinese with English abstract).
- Li J X, Li G M, Qin K Z, Xiao B. 2011a. High temperature primary magmatic fluid directly exsolved from magma at Duobuza gold-rich porphyry copper deposit, Northern Tibet. Geofluids, 11, 134~143.
- Li J X, Qin K Z, Li G M, Xiao B, Zhao J X, Chen L. 2011b. Magmatic-hydrothermal evolution of the Cretaceous Duolong gold-rich porphyry copper deposit in the Bangongco metallogenetic belt, Tibet: evidence from U-Pb and $^{40}\text{Ar}/^{39}\text{Ar}$ geochronology. Journal of Asian Earth Sciences 41 (6), 525~536.
- Li G M, Li J X, Qin K Z, Duo J, Zhang T P, Xiao B, Zhao J X. 2012. Geology and hydrothermal alteration of the Duobuza gold-rich porphyry copper district in the Bangongco metallogenetic belt, northwestern Tibet. Resource Geology. 62, 99~118.
- Li J X, Qin K Z, Li G M, Xiao B, Zhao J X, Cao M J, Chen L. 2013. Petrogenesis of ore-bearing porphyries from the Duolong porphyry Cu-Au deposit, central Tibet: evidence from U-Pb geochronology, petrochemistry and Sr-Nd-Hf-O isotope characteristics. Lithos 160~161, 216~227.
- Li J X, Qin K Z, Li G M, Richards J P, Zhao J X, Cao M J. 2014a. Geochronology, geochemistry, and zircon Hf isotopic compositions of Mesozoic intermediate-felsic intrusions in central Tibet: Petrogenetic and tectonic implications. Lithos. 198~199, 77~91.
- Li S M, Zhu D C, Wang Q, Zhao Z D, Sui Q L, Liu S A, Liu D, Mo X X. 2014b, Northward subduction of Bangong-Nujiang Tethys: Insight from Late Jurassic intrusive rocks from Bangong Tso in western Tibet. Lithos, 205: 284~297.
- Liu Shen, Hu Ruizhong, Chi Xiaoguo, Li Cai, Feng Caixia and Wang Tianwu. 2003. Geochemical Characteristics and petrogenesis of the post-collision ultra potassium volcanic rocks in Qiangtang rock zone. Geotectonica et Metallogenica, 27(2): 167~175. (in Chinese with English abstract).
- Liu Y S, Gao S, Hu Z C, Gao C G, Zong K Q and Wang D B. 2010. Continental and oceanic crust recycling-induced melt-peridotite interactions in the Trans-North China Orogen: U-Pb dating, Hf isotopes and trace elements in zircons from mantle xenoliths. Journal of Petrology, 51(1-2):537~57
- Ma C Q, Li Z C, Ehlers C, Yang K G, Wang RJ. 1998. A post-collisional magmatic plumbing system: Mesozoic granitoid plutons from the Dabieshan high-pressure and ultrahigh-pressure metamorphic zone, east-central China. Lithos, 45(1~4):431~456.
- Maniar P D, Picco Publi li P M. 1989. Tectonic discrimination of granitoids. Geological Society of America Bulletin, 101(5): 635~643.
- Matte P, Taponnie P, Arnaud N, Bourjot L, Avouac J P, Vidal P H, Liu Q, Pan Y S, Wang Y. 1996. Tectonics of western Tibet, between the Tarim and the Indus. Earth and Planetary Science Letters, 142:311~320.
- McCarron J J, Smellie J L. 1998, Tectonic implications of fore-arc magmatism and generation of high-magnesian andesites: Alexander Island, Antarctica. Journal of the Geological Society, 155:269~280.
- Middlemost E A K., 1994. Naming materials in the magma/igneous rock system. Earth-Science Reviews. 37, 215~224.
- Miller C, Schuster R, Klotzli U, Grasemann B. 1999. Post-collisional potassic and ultra-potassic magmatism in SW Tibet, geochemical, Sr-Nd-Pb-O isotopic constraints for mantle source characteristics and petrogenesis. Journal of petrology, 83:5361~5375.

- Morrison G W. 1980. Characteristics and tectonic setting of the shoshonite rock association. *Lithos*, 13(1):97~108.
- Mo Xuanxue, Deng Jinfu, Dong Fangliu, Yu Xuehui, Wang Yong, Zhou Su, Yang Weiguang. 2001. Volcanic Petrotectonic Assemblages in Sanjiang Orogenic Belt, SW China and Implication for Tectonics. *Geological Journal of China Universities*, 7 (2): 121 ~ 138. (in Chinese with English abstract).
- Müller D, Rock NMS and Groves DI. 1992. Geochemical discrimination between shoshonitic and potassic volcanic rocks in different tectonic settings: A pilot study. *Mineralogy and Petrology*, 46(4):259~289.
- Nasdala L, Hofmeister W, Norberg N, Martinson J M, Corfu F, Dörr W, Kamo S L, Kennedy A K, Kronz A, Reiners P W, Frei D, Kosler J, Wan Y, Götze J, Häger T, Kröner and Valley J W. 2008. ZirconM257-a homogeneous natural reference material for the ion microprobe U-Pb analysis of zircon. *Geostandards and Geoanalytical Research*, 32(3), 247 ~ 265. Shand S J. 1943.
- Noll P D, Newson H E, Leeman W P, Ryan JG. The role of hydrothermal fluids in the production of subduction zone magmas: evidence from siderophile and chalcophile trace elements and boron. *Geochimica et Cosmochimica Acta*, 1996, 60: 587~611.
- Pan Guitang, Zhu Dicheng, Wang Liquan, Liao Zhongli, Geng Quanru, Jiang Xinsheng. 2004. Bangong Lake-Nu River suture zone—the northern boundary of Gondwanaland: Evidence from geology and geophysics. *Earth Science Frontiers*, 11(4):371~382. (in Chinese with English abstract).
- Patchett P J, Kouvo O, Hedge C E, Tatsumoto M. 1981. Evolution of continental crust and mantle heterogeneity: Evidence from Hf isotopic. *Contributions to Mineralogy and Petrology*, 78:279 ~ 297.
- Pearce JA. 1982. Trace element characteristics of lavas from destructive plate boundaries. // Andesites: orogenic andesites and related rocks. New York: John Wiley and Sons. 525~548.
- Pearce J A. 1983. Role of the sub-continental lithosphere in magma genesis at active continental margins. In: Hawkesworth CJ and Norry MJ (eds.), *Continental Basalts and Mantle Xenoliths*. Shiva, Nantwich, 230~249.
- Pearce J A, Deng, W, 1988. The ophiolites of the Tibet geotraverse, Lhasa to Golmud (1985) and Lhasa to Kathmandu (1986). *Philosophical Transactions of the Royal Society A*327, 215~238.
- Peccerillo A, Taylor SR, 1976. Geochemistry of Eocene calc-alkaline volcanic-rocks from Kastamonu district, northern Turkey. *Contributions to Mineralogy and Petrology* 58, 63 ~ 81.
- Qiu Ruizhao, Zhou Su, Deng Jinfu, Li Jinfu, Xiao Qinghu, Cai Zhiyong. 2004. Dating of gabbro in the Shemalagou ophiolite in the western segment of the Bangong Co-Nujiang ophiolite belt, Tibet—with a discussion of the age of the Bangong Co-Nujiang ophiolite belt. *Geology in China*, 31(3):262~268. (in Chinese with English abstract).
- Qu X M, Hou Z Q, Li Y G. 2004. Melt components derived from a subducted slab in late orogenic ore-bearing porphyries in the Gangdese copper belt, southern Tibetan plateau. *lithos*74:131 ~148
- Qu Xiaoming, Xin Hongbo. 2006. Ages an tectonic environment of the Bangong Co porphyry copper belt in western Tibet, China. *Geological Bulletin of China*, 25(7):792~799(in Chinese with English abstract).
- Ratajeski K, Sisson T W, Glazner A F. 2005. Experimental and geochemical evidence for derivation of the El Capitan Granite, California, by partial melting of hydrous gabbroic lower crust. *Contributions to Mineralogy and Petrology*, 149 (6): 713 ~734.
- Richards J P. 2003. Tectono-magmatic precursors for porphyry Cu-(Mo-Au) deposit formation. *Economic Geology*, 98: 1515 ~1533.
- Rollison HR. 2000. Petro-geochemistry. In: Yang XM, Yang XY and Chen SX (translate). Hefei: Press of University of Science and Technology of China, 186~187 (in Chinese).
- Ramos V. Plate tectonic setting of the Andean cordillera. *Episodes*, 1999, 22: 183~190.
- She Hongquan, Li Jinwen, Ma Dongfang, Li Guangming, Zhang Dequan, Feng Chengyou, Qu Wenjun and Pan Guitang. 2009. Molybdenite Re-Os and SHRIMP zircon U-Pb dating of Duobuza porphyry copper deposit in Tibet and its geological implications. *Mineral deposits*, 28(6):737~746. (in Chinese with English abstract).
- Shi R D. 2007. SHRIMP dating of the Bangong Lake SSZ-type ophiolite: Constraints on the closure time of ocean in the Bangong Lake-Nujiang River, northwestern Tibet. *Chinese Science Bulletin*, 52(7):936~941
- Sui Q L, Wang Q, Zhu D C, Zhao Z D, Chen Y, Santosh M, Hu Z C, Yuan H L, Mo X X. 2013. Compositional diversity of ca. 110 Ma magmatism in the northern Lhasa Terrane, Tibet: implications for the magmatic origin and crustal growth in a continent-continent collision zone. *Lithos* 168, 144~159.
- Sun S S, McDonough W E, 1989. Chemical and isotopic systematics of oceanic basalts: implications for mantle composition and processes. In: Saunders, A. D., Norry, M. J. (Eds.), *Magmatism in the Ocean Basins*; Geological Society of London, Specialcation, pp. 313~345.
- Sun Zhenming, Ren Yunsheng, Li Cai, Li Xingkui, Wang Ming, Fan Jianjun. 2015. Fluid inclusion characteristics and ore genesis of the Rongna Cu(Au) Deposit in the western part of the Bangong Lake-Nujiang Suture Zone Tibet. *Acta Geologica Sinica*, 89(3):608~617.
- Tang Juxing, Sun Xinguo, Ding Shuai, Wang Qin, Wang Yiyun, Yang Chao, Chen Hongqi, Li Yanbo, Li Yubin, Wei Lujie, Zhang Zhi, Song Junlong Yang Huanhuan, Duan Jilin, Gao Ke, Fang Xiang, Tan Jiangyun. 2014. Discovery of the

- Epithermal Deposit of Cu (Au-Ag) in the Duolong Ore Concentrating Area, Tibet. *Acta Geoscientica Sinica*, 35(1): 6 ~10(in Chinese with English abstract).
- Tarney J and Jones CE. 1994. Trace element geochemistry of orogenic igneous rocks and crustal growth models. *Journal of the Geological Society*, 151(5):855~868.
- Wang Qin, Tang Juxing, Fang Xiang, Lin Bin, Song Yang, Wang Yiyun, Yang Huanhuan, Yang Chao, Li Yanbo, Wei Lujie, Feng Jun, Li Li. 2015. Petrogenetic setting of andesites in Rongna ore block, Tiegelong Cu (Au-Ag) deposit, Duolong ore concentration area, Tibet; Evidence from zircon U-Pb LA-ICP-MS dating and petrogeochemistry of andesites. *Geology in China*, 42(5):1324~1336(in Chinese with English abstract).
- Wilkinson JJ. 2013. Triggers for the formation of porphyry ore deposits in magmatic arcs. *Nature Geoscience*. 6: 917~925.
- Wu Fuyuan, Li Xianhua, Zheng YongFei and Gao Shan. 2007. Lu-Hf isotopic systematic and their applications in petrology. *Acta petrologica Sinica*, 23(2):185~220. (in Chinese with English abstract).
- Wu Genyao, Wang Xiaopeng and Zhong Dalai. 1999. Early Cretaceous Andean-type arc volcanics in SE Xizang, China. *Acta Petrologica Sinica*, 15(3): 422~ 429. (in Chinese with English abstract).
- Xin Hongbo, Qu Xiaoming, Wang Ruijiang, Liu Hongfei, Zhao Yuanyi and Huang Wei. 2009. Geochemistry and Pb, Sr, Nd isotopic features of ore-bearing porphyries in Bangong Lake porphyry copper belt, western Tibet. *Mineral deposits*, 28(6): 785~792. (in Chinese with English abstract).
- Yang Chao, Tang Juxing, Wang YiYuan, Yang Huanhuan, Wang Qin, Sun Xinguo, Feng Jun, Yin Xianbo, Ding Shuai, Fang Xiang, Zhang zhi and Li Yubin. 2015. Fluid and Geological characteristics researchers of Southern Tiegelong epithermal porphyry Cu_Au Deposit in Tibet. *Mineral deposits*, 33(6): 1287~1305. (in Chinese with English abstract).
- Yin A., Harrison T. M., 2000. Geological evolution of the Himalayan-Tibetan orogen. *Annual Review of Earth and Planetary Sciences* 28,211~280.
- Yuan H L, Gao S, Dai M N, Zong C L, Günther D, Fontaine G H, Liu X M, and Diwu C. R. 2008 Simultaneous determinations of U-Pb age, Hf isotopes and trace element compositions of zircon by excimer laser-ablation quadrupole and multiple-collector ICP-MS. *Chem. Geol.* 247, 100~118.
- Zhang Liangliang, Zhu Dicheng, Zhao Zhidan, Dong Guochen, Mo Xuanxue, Guan Qi, Liu Ming, Liu Meihua. 2010. Petrogenesis of magmatism in the Baerda region of northern gangdese, Tibet: Constraints from geochemistry, geochronology and Sr-Nd-Hf isotopes. *Acta Geologica Sinica*, 27(7):1938~1948. (in Chinese with English abstract).
- Zhang K J, Xia B D, Wang G M, Li Y T, Ye H F. 2004. Early Cretaceous stratigraphy, depositional environments, sandstone provenance, and tectonic setting of central Tibet, western China. *GSA Bulletin*, 116(9~10):1202~1222.
- Zhu D C, Mo X X, Niu Y L, Zhao Z D, Wang L Q, Liu Y S, Wu F Y, 2009. Geochemical investigation of Early Cretaceous igneous rocks along an east-west traverse throughout the central Lhasa Terrane, Tibet. *Chemical Geology* 268, 298 ~312.
- Zhu DC, Zhao ZD, Niu YL, Mo XX, Chung SL, Hou ZQ, Wang LQ, Wu FY, 2011. The Lhasa terrane: record of a microcontinent and its histories of drift and growth. *Earth and Planetary Science Letters* 301, 241~255.
- Zhu Dicheng, Pan Guitang, Mo Xuanxue, Wang Liquan, Zhao Zhidan, Liao Zhongli, Geng Quanru, Dong Guochen. 2006a. Identification of the Mesozoic OIB-type basalts in central Qinghai-Tibetan Plateau: geochronology, geochemistry and their tectonic setting. *Acta Geol. Sinica* 80, 1312 ~ 1328 (in Chinese with English abstract).
- Zhu Dicheng, Pan Guitang, Mo Xuanxue, Wang Liquan, Liao Zhongli, Zhao Zhidan, Dong Guochen and Zhou ChengYong. 2006b. Late Jurassic-Early Cretaceous geodynamic setting in middle-northern Gangdese: new insights from volcanic rocks. *Acta Petrologica Sinica* 22, 534~546. (in Chinese with English abstract).
- Zhu Dicheng, Mo Xuanxue, Zhao Zhidan, Xu Jifeng, Zhou Changyong, Sun Chenguang, Wang Liquan, Chen Haihong, Dong Guochen, Zhou Su. 2008a. Zircon U-Pb geochronology of Zenong group volcanic rocks in Coqen area of the gangdese, Tibet and tectonic significance. *Acta Geologica Sinica*. 24(3): 401~412. (in Chinese with English abstract).
- Zhu Dicheng, Pan Guitang, Wang Liquan, Mo Xuanxue, Zhao Zhidan, Zhou Changyong, Liao Zhongli, Dong Guochen, Yuan Sihua. 2008b. Spatial-temporal distribution and tectonic setting of Jurassic magmatism in the Gangdese belt, Tibet, China. *Geological Bulletin of China*, 27(4): 458 ~ 468 (in Chinese with English abstract).
- Zhu Xiangping, Chen Huaan, Liu Hongfei, Ma Dongfang, Li Guangming, Zhang Hong, Liu Chaoqing, Wei Lujie. 2015. Geochronology and geochemistry of porphyry copper deposit, Tibet and their metallogenesis significance. *Acta Geologica Sinica*. 89(1):109~128 (in Chinese with English abstract).
- Zhu X P, Li G M, Chen H'A, Ma D F, Huang H X. 2015. Zircon U-Pb, Molybdenite Re-Os and K-feldspar 40Ar/39Ar Dating of the Bolong Porphyry Cu-Au Deposit, Tibet, China. *Resource Geology*, 65(2): 122~135

参 考 文 献

- 鲍佩声,肖序常,苏犁,王军. 2007. 西藏洞错蛇绿岩的构造环境:岩石学、地球化学和年代学制约. *中国科学:D辑:地球科学*, 37 (3):298~307.
- 常青松,朱弟成,赵志丹,董国臣,莫宣学,刘勇胜,胡兆初. 2011. 西藏羌塘南缘热那错早白垩世流纹岩锆石 U-Pb 年代学和 Hf 同位素及其意义. *岩石学报*, 27(7):2034~2044.
- 陈华安,祝向平,马东方,黄瀚霄,李光明,李玉彬,李玉昌,卫鲁杰,

- 刘朝强. 2013. 西藏波龙斑岩铜金矿床成矿斑岩年代学岩石化学特征及其成矿意义. 地质学报, 87(10): 1~19.
- 陈越, 朱弟成, 张志丹, 张亮亮, 刘敏, 于枫, 管琪, 莫宣学. 2010. 西藏北冈底斯巴木错安山岩的年代学、地球化学及岩石成因. 岩石学报, 26(7): 2193~2206.
- 崔宁, 邢树文, 肖克炎, 丁建华. 2016. 班公湖—怒江 Cu-Au-Fe-Li 多金属成矿带主要地质成矿特征及潜力分析. 地质学报, 90(7): 1623~1635.
- 邓晋福, 肖庆辉, 苏尚国, 刘翠, 赵国春, 吴宗纂, 刘勇. 2007. 火成岩构造组合与环境: 讨论. 高校地质学报, 13(3): 392~402.
- 董国臣, 莫宣学, 赵志丹, 朱弟成, 宋云涛, 王磊. 2008. 西藏冈底斯南带辉长岩及其所反映的壳幔作用信息. 岩石学报, 24(2): 203~210.
- 段志明, 李光明, 张晖, 段瑶瑶. 2013. 西藏班公湖—怒江缝合带北缘多龙矿集区晚三叠世—侏罗纪增生杂岩结构及其对成矿地质背景的约束. 地质通报, 32(5): 742~750.
- 方向, 唐菊兴, 宋杨, 杨超, 丁帅, 王艺云, 王勤, 孙兴国, 李玉彬, 卫鲁杰, 张志, 杨欢欢, 高轲, 唐攀. 2015. 西藏铁格隆南超大型浅成低温热液铜(金、银)矿床的形成时代及其地质意义. 地球学报, 36(2): 168~176.
- 郭铁鹰, 梁定益, 张宜智. 1991. 西藏阿里地质. 武汉: 中国地质大学, 1~106.
- 侯可军, 李延河, 田有荣. 2009. LA-MC-ICP-MS 锆石微区原位 U-Pb 定年技术. 矿床地质, 28(4): 481~492.
- 黄玉, 朱弟成, 赵志丹, 张亮亮, Don Depalolo, 胡兆初, 袁洪林, 莫宣学. 2012. 西藏北部拉萨地块那曲地区约 113Ma 安山岩岩石成因与意义. 岩石学报, 28(5): 1603~1614.
- 李光明, 李金祥, 秦克章, 张天平, 肖波. 2007. 西藏班公湖带多不杂超大型富金斑岩铜矿的高温高盐高氧化成矿流体: 流体包裹体证据. 岩石学报, 23(05): 935~952.
- 李金祥, 李光明, 秦克章, 肖波. 2008. 班公湖带多不杂富金斑岩铜矿床斑岩火山岩的地球化学特征与时代: 对成矿构造背景的制约. 岩石学报, 24(3): 531~543.
- 刘燊, 胡瑞忠, 迟效国, 李才, 冯彩霞, 王天武. 羌塘岩带碰撞后超钾质火山岩地球化学特征及成因探讨. 大地构造与成矿学, 2003, 27(2): 165~175.
- 莫宣学, 邓晋福, 董方浏, 喻学惠, 王勇, 周肃, 杨伟光. 2001. 西南三江造山带火山岩一构造组合及其意义. 高校地质学报, 7(2): 121~138.
- 潘桂棠, 朱弟成, 王立全, 廖忠礼, 耿全如, 江新胜. 2004. 班公湖—怒江缝合带作为冈瓦纳大陆北界的地质地球物理证据. 地学前缘, 11(4): 371~382.
- 邱瑞照, 周肃, 邓晋福, 李金发, 肖庆辉, 蔡志勇. 2004. 西藏班公湖—怒江西段舍马拉沟蛇绿岩中辉长岩年龄测定——兼论班公湖—怒江蛇绿岩带形成时代. 中国地质, 31(3): 262~268.
- 曲晓明, 辛洪波. 2006. 藏西班公湖斑岩铜矿带的形成时代与成矿构造环境. 地质通报, 25(7): 792~799.
- 余宏全, 李进文, 马东方, 李光明, 张德全, 丰成友, 屈文俊, 潘桂棠. 2009. 西藏多不杂斑岩铜矿床辉钼矿 Re-Os 和锆石 U-Pb SHRIMP 测年及地质意义. 矿床地质, 28(6): 737~746.
- 孙振明, 任云生, 李才, 李兴奎, 王明, 范建军. 2015. 西藏班—怒带西段荣那铜(金)矿床流体包裹体特征及矿床成因. 地质学报, 89(3): 608~617.
- 唐菊兴, 孙兴国, 丁帅, 王勤, 王艺云, 杨超, 陈红旗, 李彦波, 李玉彬, 卫鲁杰, 张志, 宋俊龙, 杨欢欢, 段吉琳, 高轲, 方向, 谭江云. 2014. 西藏多龙矿集区发现浅成低温热液型铜(金银)矿床. 地球学报, 1: 6~10.
- 王勤, 唐菊兴, 方向, 林彬, 宋扬, 王艺云, 杨欢欢, 杨超, 李彦波, 卫鲁杰, 冯军, 李力. 2015. 西藏多龙矿集区铁格隆南铜(金银)矿床荣那矿段安山岩成岩背景: 来自锆石 U-Pb 年代学、岩石地球化学的证据. 中国地质, 42(5): 1324~1336.
- 吴福元, 李献华, 郑永飞, 高山. 2007. Lu-Hf 同位素体系及其岩石学应用. 岩石学报, 23(2): 185~220.
- 吴根耀, 王晓鹏, 钟大赉. 1999. 藏东南地区早白垩世的安第斯型弧火山岩. 岩石学报, 15(3): 422~429.
- 辛洪波, 曲晓明, 王珠江, 刘鸿飞, 赵元艺, 黄玮. 2009. 藏西班公湖斑岩铜矿带成矿斑岩地球化学及 Pb-Sr-Nd 同位素特征. 矿床地质, 28(6): 785~792.
- 杨超, 唐菊兴, 王艺云, 杨欢欢, 王勤, 孙兴国, 冯军, 印贤波, 丁帅, 方向, 张志, 李玉彬. 2014. 西藏铁格隆南浅成低温热液型一斑岩型 Cu-Au 矿床流体及地质特征研究. 矿床地质, 6: 1287~1305.
- 张亮亮, 朱弟成, 赵志丹, 董国臣, 莫宣学, 管琪, 刘敏, 刘美华. 2011. 西藏申扎早白垩世花岗岩类: 板片断离的证据. 岩石学报, 27(7): 1938~1948.
- 朱弟成, 潘桂棠, 莫宣学, 王立全, 赵志丹, 廖忠礼, 耿全如, 董国臣. 2006a. 青藏高原中部中生代 OIB 型玄武岩的识别年代学、地球化学及其构造环境. 地质学报, 80(9): 1312~1328.
- 朱弟成, 潘桂棠, 莫宣学, 王立全, 廖忠礼, 赵志丹, 董国臣, 周长勇. 2006b. 冈底斯中北部晚侏罗—早白垩世地球动力学环境: 火山岩约. 岩石学报, 2(3): 534~546.
- 朱弟成, 莫宣学, 张志丹, 许继峰, 周长勇, 孙晨光, 王立全, 陈海红, 董国臣, 周肃. 2008a. 西藏冈底斯带措勤地区则弄群火山岩锆石 U-Pb 年代学格架及构造意义. 岩石学报, 24(3): 401~412.
- 朱弟成, 潘桂棠, 王立全, 莫宣学, 赵志丹, 周长勇, 廖忠礼, 董国臣, 袁四化. 2008b. 西藏冈底斯带中生代岩浆岩的时空分布和相关问题的讨论. 地质通报, 27(9): 1535~1550.
- 祝向平, 陈华安, 刘鸿飞, 马东方, 李光明, 张红, 刘朝强, 卫鲁杰. 2015. 西藏拿若斑岩铜金矿床成矿斑岩年代学、岩石化学特征及其成矿意义. 地质学报, 1: 109~128.

Petrogenesis, Zircon U-Pb Geochronology and Sr-Nd-Hf Isotopes of the Intermediate-felsic Volcanic Rocks from the Duolong deposit in the Bangonghu-Nujiang Suture Zone, Tibet, and Its Tectonic Significance

WEI Shaogang¹⁾, TANG Juxing²⁾, SONG Yang²⁾, LIU Zhibo²⁾, WANG Qin³⁾,
LIN Bin²⁾, HE Wen¹⁾, FENG Jun⁴⁾

1) School of Earth Science and Resources, China University of Geosciences, Beijing, 10083, China;

2) Institute of Mineral Resources, Chinese Academy of Geological Sciences, Beijing, 10037, China;

3) Chengdu University of Technology, Chengdu, 610059, China;

4) Tibet JinlongMining Co., Ltd., Lhasa, 850000, China

Abstract

The Bangonghu-Nujiang suture zone in Tibet of China, has been is an important porphyry copper gold metallogenic belt, with superior geological condition of mineralization, The Duolong ore-concentrated deposit, the first superlarge epithermal porphyry Cu-Au deposit discovered in the western Bangonghu-Nujiang suture zone, is widely covered with plenty of effusive volcanic rocks. However, the petrogenesis, magma source and geodynamic setting of the granitoids are still constrained loosely. In this paper, LA-ICP-MS zircon date yields U-Pb age of 108.2 ± 2.6 Ma (MSWD = 0.39) for the dacite, regarding to the similar geochronological data of 109.3 ± 2.2 Ma (MSWD = 1.70) for the rhyolite. The dacite and rhyolite are characterized by high silica ($\text{SiO}_2 = 60.89\% \sim 72.00\%$), potassium-rich ($\text{K}_2\text{O} = 3.08\% \sim 5.53\%$), alkali-rich ($\text{K}_2\text{O} + \text{Na}_2\text{O} = 6.88\% \sim 8.96\%$), peralkaline to peraluminous ($\text{A/CNK} = 0.92 \sim 1.28$) and High calc-alkaline to shoshonitic. The rocks are systematically more enriched in large-ion lithophile elements (LILE: Th, U, K, Pb and Rb) and LREE, relatively depleted in high strength elements (HFSE: Ta, Nb, Ti and Zr) and HREE. Total Concentration of REE range from $141.52 \times 10^{-6} \sim 236.05 \times 10^{-6}$, with LREE/HREE of $8.54 \sim 9.30$, $\text{La}_{\text{N}}/\text{Yb}_{\text{N}}$ of $10.42 \sim 11.05$ and middle negative Eu anomalies ($\delta\text{Eu} = 0.65 \sim 0.80$). Besides, trace elements compositions indicate that the magma is contaminated by crustal mantle when it rises and The isotopes of these rocks are characterized by high $(^{87}\text{Sr}/^{86}\text{Sr})_i$ (from 0.7050 to 0.7053), low $(^{143}\text{Nd}/^{144}\text{Nd})_i$ (from 0.5124 to 0.5126), low $\epsilon_{\text{Nd}}(t)$ (from -1.51 to 1.29). The positive $\epsilon_{\text{Hf}}(t)$ values of zircons from rhyolite whose second stage Hf mode mean ages are 288.0 Ma vary from +11.6 to +15.5, contrasted with $\epsilon_{\text{Hf}}(t)$ values of +3.4 ~ +8.0 from dacite whose second stage Hf mode mean ages are 813.1 Ma. Based on the above discussions, we proposed that the geochemical characteristics of these volcanic rocks are consistent with those of arc-type magmas worldwide and the arc volcanic rocks magma were all generated by partial melting of mantle wedges replaced by the fluid which is formed the dehydration of the oceanic crust subduction plate, and its rock-forming resulted from the mixing between the juvenile lower crust-derived melts and mantle-derived mafic melts under the background of Bangonghu-Nujiang Tethys subducting northward to Qiangtang massif. In addition, the volcanic activity suggests Bangonghu-Nujiang ocean was subducting at least during approximate 108 ~ 109 Ma, and the closure time of this ocean should be later than early Cretaceous (108 ~ 109 Ma), which is different from early recognition of closure time of late Jurassic to early-Cretaceous.

Key words: Closure time; Island-arc volcano rock; Early Cretaceous; Duolong ore-concentrated district; western Bangonghu-Nujiang suture zone; Tibet